Postprint of: Kolerski T., Assessment of the ice jam potential on regulated rivers and reservoirs with the use of numerical model results, COLD REGIONS SCIENCE AND TECHNOLOGY, Vol. 191, iss. 11 (2021), 103372, DOI: 10.1016/j.coldregions.2021.103372

Assessment of the ice jam potential on regulated rivers and reservoirs with the use of numerical model results

Tomasz Kolerski

Gdańsk University of Technology, Faculty of Civil and Environmental Engineering,
Narutowicza 11/12, 80-233 Gdańsk, Poland
tomasz.kolerski@pg.edu.pl

Abstract

This study presents an attempt at estimating the jam potential on rivers with significant anthropogenic intervention in the course or flow characteristics of the river. The DynaRiCE model was used for forecasting both the place and time of an ice jam occurrence. In this modified method, two ice parameters are subjected to analysis, namely the relative ice-to-water velocity ($^{v_i}/_{v_w}$),and the ice thickness to single floe thickness ($^{\eta_i}/_{\eta_0}$). Both variables were analyzed at two locations; first spot is the Odra River near Słubice-Frankfurt bridge (between 581 and 586 km), and the second is the Vistula section between the existing Włocławek dam (674.75 river km) and the planned Siarzewo dam (706.38 river km), covering a 31.6 km reach. Once the model is implemented in the selected areas, the numerical simulations were processed and the obtained results were analyzed in terms of ice accumulation and jamming. The results on both rivers shown some potential of ice jamming, due to the planned engineering works. In the case of the Odra river, it was indicated that ice jam potential increased during the ice run of high concentration in the average flow conditions. For the Vistula river two locations for ice jamming were designated and for both of the points an increase of the ice thickness by about 60 % from the initial, single flow thickness was observed. Also in this case, the area-averaged ice velocity in an initially specified location drops below 15% of the average water

velocity in that area. According to the used methodology, both cases are classified as 'ice jam probable' type.

Keywords: ice dynamics; ice jams; river engineering; Odra River; Vistula River

1 Introduction

A common issue in engineering practice is to estimate the ice congestion and jamming potential of rivers due to planned river engineering works or new run-of-river reservoirs and diversion dams. The task most often comes down to determining to what extent hydrotechnical structures will affect ice transport, and whether or not they will not stop the ice run during freeze-up and during spring or mid-winter breakup. In order to consider the fragmented ice cover at locations where border ice has grown across the river or where man-made structures form a surface barrier, drifting ice can accumulate and progress upstream (Svensson et al., 1989). This issue is not a trivial task and above all requires the determination of the impact of hydro-engineering structures on the ice dynamics. Analyses should additionally take into account other factors affecting ice flow; i.e., wind speed and direction, hydrological and meteorological factors, as well as flow regulation through diversion structures (Ashton, 1978; Grześ, 1991; Lal and Shen, 1991; White, 1999).

Historical observations provide a vision for researchers to know the severity of the ice-related flood damaging. Floods are most likely to occur on rivers that have experienced flooding in the past. Despite this, potential flood hazard may be unknown to some residents and local authorities, due to the long intervals of flood or the resident's recent arrival in the area (Kovachis et al., 2017). It is needed to be considered that reoccurring the ice jams may cause the geometric impacts on the river basins (Boucher et al., 2009). From an ecosystem perspective, a longer-term view may be more important than annual predictability (Timoney et al., 1997). Having access to data set, it is possible to illustrate how ice regime characteristics may have varied through time and space within the cold-region watercourse and examine some of the potential geomorphic responses associated with ice jam dynamics (Boucher et al., 2012). An important consideration is the inherent uncertainty in these

data sets, which must be factored into assessment of ice-jam flood history (Wolfe et al., 2020). Although, statistical information of ice processes helps to understand general trends in ice cover formation and ice movement, the complexity of the processes makes it nearly impossible to achieve a higher accuracy level (Kolerski, 2018). To predict water levels that can potentially occur as a result of ice jamming, it is necessary to apply one of several numerical models that are available. Regardless of which model is selected for application, certain hydraulic and morphologic data sets are needed (Beltaos and Burrell, 2015). However, by utilizing existing theories, a mathematical model of these processes can be developed. Such model can be used to provide a continuous description of river ice development based on a limited amount of field data. The model can also assist engineers in evaluating the possible beneficial and detrimental consequences of ice-control structures and flow regulation (Lal and Shen, 1991).

Following the model selection, the results of the modeling run, as well as scenarios of ice jams of different length and locations can be concluded (Beltaos, 2018). To quantify which factor influences the formation of ice jamming the most, a local parameter sensitivity analysis can be carried out to calculate the sensitivity of different parameters on ice jam flooding (Das and Lindenschmidt, 2020). In other words, a sensitivity analysis can be performed to evaluate changes in model predictions resulting from changes in several model input parameters. The parameters like: river flow rate, locations of ice jam formation, ice supply volume entering from upstream, downstream water level, and underside roughness (i.e. Manning's coefficient) of the ice cover and jam (Liu and Shen, 2005).

In recent years, knowledge about ice processes on rivers has been significantly improved, which is reflected in the developed mathematical models for simulating flow in rivers in winter conditions. The initial concept of the static ice jam theory, first developed by (Pariset et al., 1966; Pariset and Hauser, 1961) is based on a static balance of floating ice. It was further developed by (Uzuner and Kennedy, 1976, 1974) and used in a number of mathematical models. The basic ice jam stability concepts are categorized under common modular feature, and have been adopted in a number of

one-dimensional mathematical models, including the RIVJAM model developed by (Beltaos, 1983; Uzuner and Kennedy, 1976, 1974), the ICEJAM model (Flato and Gerard, 1986), RIVER1D (Hicks et al., 1992) and RIVICE (Lindenschmidt et al., 2012). Moreover, the theory behind the ice module in commercial softwares, such as the HEC RAS model or the MIKE11-ICE model closely follow static jam formulations (Brunner, 2002; Thériault et al., 2010). Since an ice jam is fully dynamic and three-dimensional in nature, modeling its occurrence and range often requires a more sophisticated approach. Therefore, Shen developed DynaRICE, a two-dimensional, depth-averaged coupled hydrodynamic and ice dynamic model of ice transport in rivers (Shen, 2010; Shen et al., 2000).

In the context of what can be defined in a broad sense as the impact assessment of river ice phenomena, one-dimensional modeling has been widely used to recreate magnitude of ice related flooding and maximum water levels reached in the river valley (Beltaos, 2003; Kandamby et al., 2010; Lindenschmidt et al., 2019; Lindenschmidt and Rokaya, 2019). In such an approach, model efficiency is significantly improved, however it assumes a regular distribution of ice velocity and thickness in a cross section. Therefore a two-dimensional model is implemented in the area, where a blockage is expected to occur (Shen and Liu, 2003; Su et al., 1997; Kolerski and Shen, 2015).

1.1 Study site

When selecting the model domain, it is important to refer to historical data and other evidence, including practical knowledge from the management of water systems and icebreaker crews. On this basis, river sections with a significant ice jam potential were determined, which were subjected to detailed numerical analyses. The assessment of the results of the numerical model in the context of the risk of an ice jam requires the area to be determined in which ice run slows noticeably and increases in concentration and thickness. Such locations are often places where the water flow diverges due to the existence of an island (Pawłowski, 2015), rapids or in the case of the channel being split into a number of distributaries (i.e. the ice jam in the St Clair delta (Kolerski and Shen, 2015)). Furthermore, a reduction in the slope of the river bed or the water level (ice inflow to a

reservoir (Rădoane et al., 2010)), a narrowness in the channel as well as the presence of engineering structures, such as bridge piers will hamper ice transport (Wang et al., 2015).

1.1.1 Odra River

A good example in ice accumulation area, is a section of the natural border river - the Odra, which is characterized in terms of ice jamming potential by the Regional Water Management Board in Szczecin (RWMB Szczecin). Information on jam-prone sections of the Odra River mainly comes from observations made during annual icebreaking operations and published reports (RWMA, 2010).

Figure 1. The catchment of the Upper and Middle sections of the Odra River

The Odra River, similar to many European rivers, was modified in the mid-18th century to establish stable conditions for navigation, and reduce bank erosion. Early river engineering works on the Odra River were mainly carried out by the construction of closure structures, built across secondary

channels to reduce floodplain conveyance and increase the main channel depth. The process was carried out until the middle of the 20th century and caused a significant reduction in large winter flooding (Mudelsee et al., 2004). However, it did not affect the ice jam potential of the river. Currently, according to the Regional Water Management Authority in Szczecin (RWMA Szczecin), the lower section of the Odra River (about 200 km), which is a natural border between Poland and Germany, has 28 ice jam prone locations extending over more than one fourth of the river.

The Polish city of Słubice is located on the banks of the Odra River, which forms the border with Germany. According to RWMA Szczecin, the river in the vicinity of the city is particularly susceptible to ice jamming. As shown in (Kolerski, 2018), this is caused by the river narrowness and an additional reduction in the cross-section triggered by a single bridge pier (Słubice-Frankfurt bridge). In recent years, the city was at risk of flooding caused by ice jamming, e.g. in February 2010. Within the Odra-Vistula Flood Management Project (OVFMP), it is planned to rehabilitate all the existing structures on a 5 km reach of the river. The proposed system of spurs is designed in the form of extensions of the existing structures which are damaged to a varying degree (Kreft and Parzonka, 2007).

Detailed river bathymetry and shoreline data measured in 2017 for the OVFMP, are used for the study. The data is considered to represent the current state of the river, which is considered to be substantially rebuilt by the construction or reconstruction of spur dikes within the OVFMP. The conditions after project implementation are taken into account in the model domain by changing the shoreline to include all the proposed structures. Within the model domain, a sub-domain was selected where a quantitative jam analysis was conducted. The area includes a river section of about 450 m long upstream of the Słubice – Frankfurt bridge. The location was selected based on the general trend in ice transport and the high potential of that area for ice jamming and accumulation. Quantitative comparisons of both the current and proposed river conditions for all the simulated cases are presented in Figure 2. The modifications are on the left bank along the whole river section, where the spur dikes are proposed.

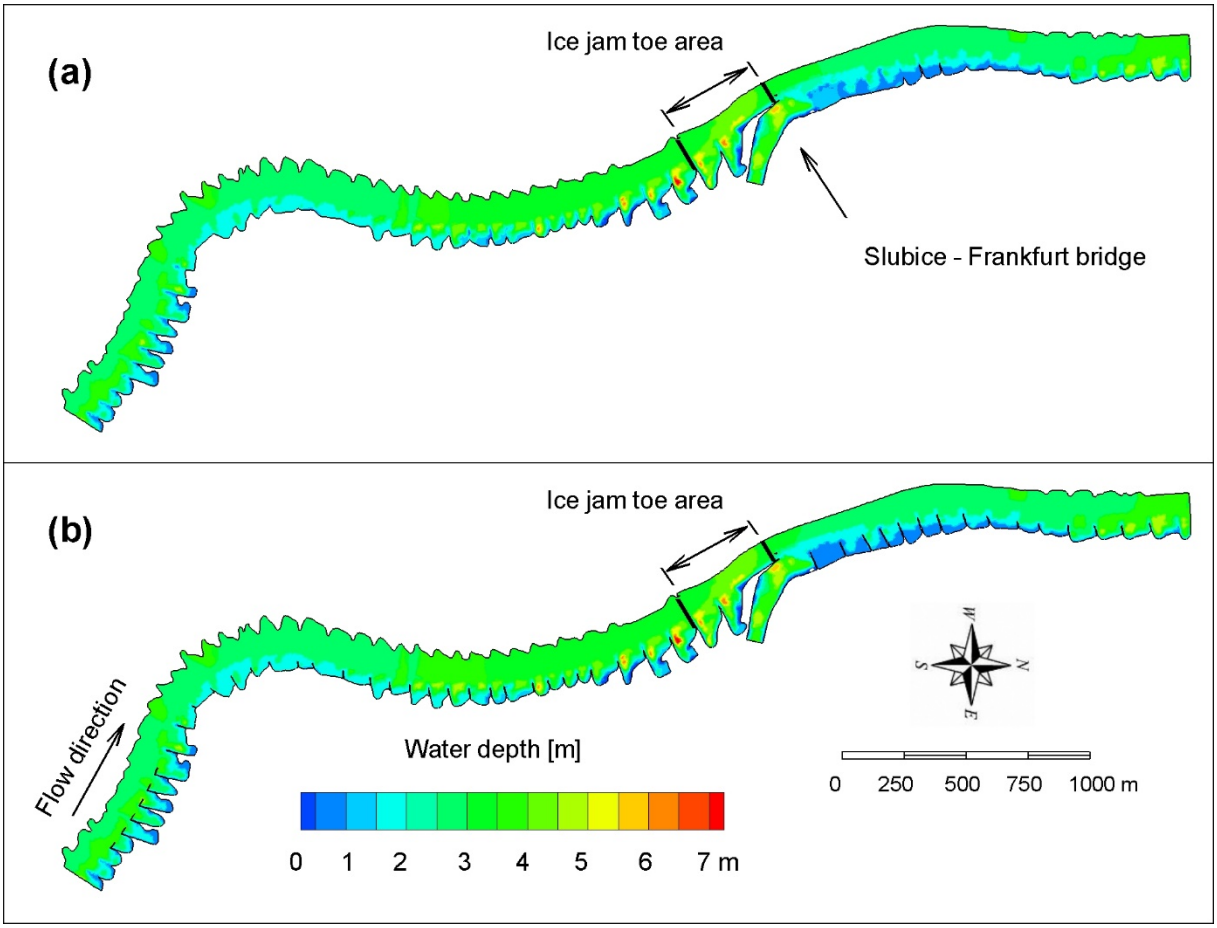

142

143 **Figure 2 Water depth at average flow (Q_w = 276 m³/s) for current** (a) **and proposed** (b) **conditions; sub-domain for**
144 **numerical jam analysis designated by arrow**

145 ### 1.1.2 Vistula River

146 If the area of interest has no historical evidence of ice jamming or its hydrodynamic features can
147 change significantly based on an executed river regulation plan, the entire reach should be included
148 in the mathematical modeling to the extent possible. Such is the case with regard to the Vistula
149 River, where a new reservoir is planned to be accomplished by the construction of a new dam in
150 Siarzewo, located at 706.4 river kilometers, which is about 30 km downstream of the existing
151 Włocławek dam.

152 Unlike the Odra, the Vistula River was regulated fragmentarily at the second half of the 19th century.
153 The river was divided between three countries, and only in the lower section (downstream of Silno –
154 see Figure 3), which formerly belonged to Prussia,)river engineering works proceeded to a large
155 extent. Currently, the river is in a state of gradual deterioration due to a lack of attention to

156 engineering works (Szymkiewicz, 2017). In addition, Włocławek diversion dam (the only reservoir
157 functioning on the Vistula River) contributed to river degradation due to a pulsed water discharge
158 which intensified the erosion downstream of the channel. From the beginning of the operation in the
159 1970s until the 1990s, the hydropower plant provided peak power demand, temporarily causing
160 rapid flow changes. The water discharge in the Vistula varied from about 400 m^3/s during off-peak
161 periods to as high as 2000 m^3/s during peak operation (Babiński, 1982; Gosztowtt, 2018).

162 Wloclawek diversion dam is a part of a low-head dam cascade developed in the 1950s (Szydlowski et
163 al., 2015). The main purpose of the concept was to improve the Polish hydropower development
164 potential and protection against flooding and water resource management for agricultural fields
165 threatened by the draught. Recently, due to economic development and resultant increased traffic
166 requirements from the Baltic Sea port (Gdańsk) to the south of the country, and removing electricity
167 inadequacy in northern Poland have stimulated welcoming the old concept of the Lower Vistula
168 Cascade operation (LVC). Siarzewo dam was first proposed at 706.38 river km, and the project is
169 currently being designed (Kolerski, 2016).

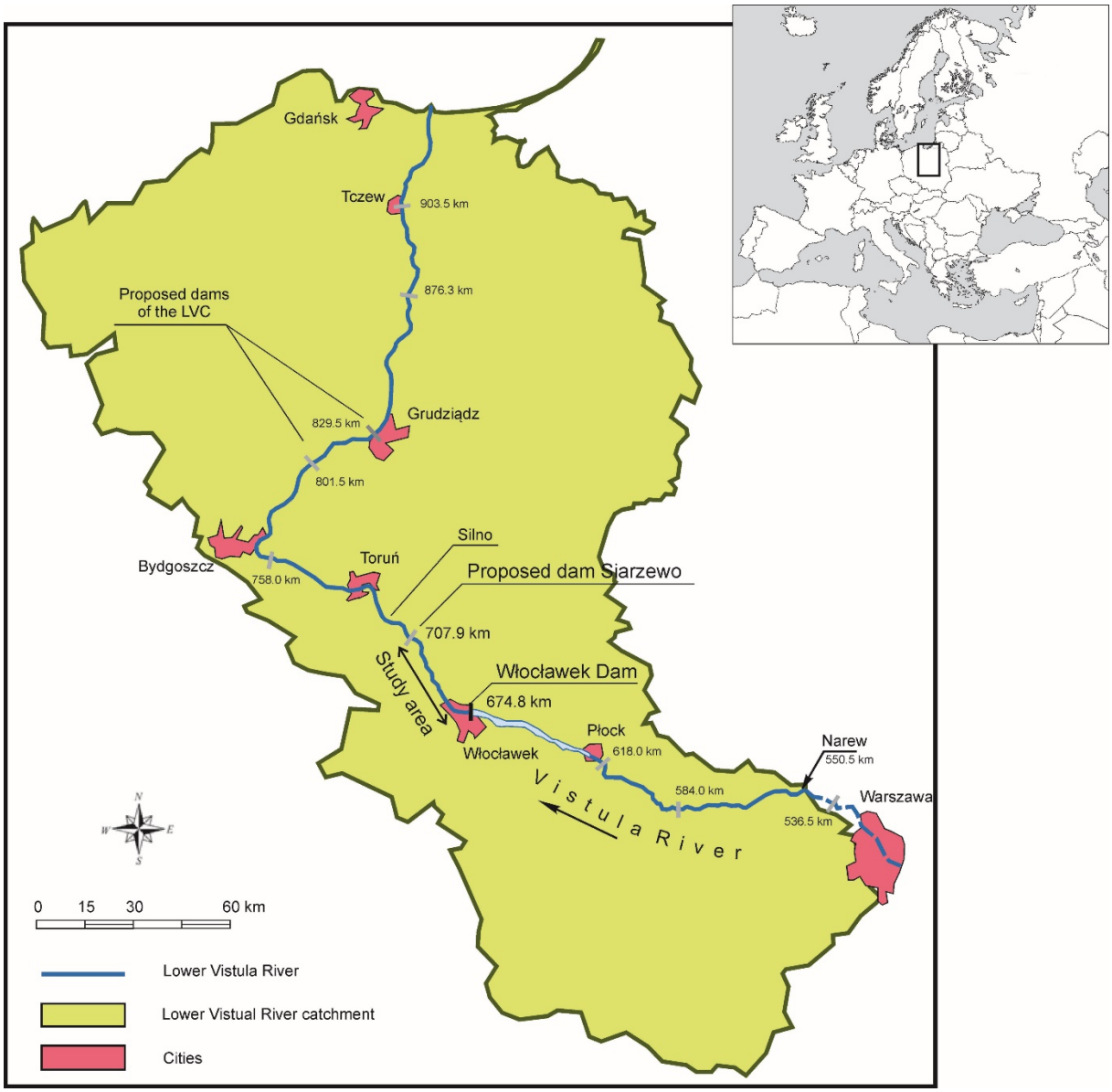

Figure 3 The Lower sections of the Vistula River—the black bars indicate locations for the proposed dams within the LVC, with river mileage

1.2 Ice condition description

1.2.1 Odra river

The ice cover on the Odra River is dominantly formed from dynamic ice accumulation. A sketch of the lower and middle Odra River is shown in Figure 4. Typically, the process of ice cover development is initiated at Dąbie Lake, where static ice cover is formed first. Next, incoming ice floes may stop at the leading edge of the ice cover on the lake or flow underneath the cover (Kolerski, 2018; Marszelewski and Pawłowski, 2019). The rate of ice cover progression in the upstream direction is affected by the water flow and ice conditions, as well as the high water levels on the Southern Baltic Sea through the

backwater effect and meteorological conditions. Ice cover formed from the accumulation of dynamic floes has a big potential for jam formation, as evidenced by yearly ice reports provided by RWMA Szczecin.

Besides natural processes, another important mechanism affecting the ice run is ice sluicing from the system of low-head reservoirs in the middle section of the Odra River (see Figure 4). It is noteworthy that a lack of coordinated icebreaking operations on the Odra and on the mentioned reservoirs could significantly increase the threat of ice jamming on the downstream section of the river. Such a situation occurred in February 2010, when ice sluicing started without prior consultation with the management of the Polish-German icebreaking operation. Breaking the ice on reservoirs and sluicing it through the spillways require an increment in discharge, which forms a surge in the downstream river section. To avoid uncontrolled breakup at the downstream section of the river, the surges must be evenly distributed over time. If ice sluicing occurs long before the icebreakers reach the edge of ice cover which is located at the upstream end of the reservoir along the river channel, the broken ice from the sluicing operation accumulates at the intact ice cover downstream of the spillway.

In the winter season of 2009-2010, 250 km of the Odra was covered by ice, and the leading edge of the ice cover reached the station of 491.4 km of the river. In the second part of February due to air temperatures above zero, the strength of the ice cover reduced; however, it still remained intact in a large portion of the river (645 - 491 river km). Regardless of the situation in the lower section of the river, an ice-sluicing operation from the reservoirs was started. Realizing the threat, icebreaker crews worked on the Odra with a great nonstop effort. On 27th February, the bridge in Słubice was reached by the icebreakers and an ice-free channel was formed. During the night of 28th February, the weakened ice cover started to collapse due to the additional ice mass released from the reservoirs, and a large amount of ice collapsed forming an uncontrolled breakup. Under these life-threatening conditions, the icebreakers were forced to flee downstream, hiding in the Warta outlet (see photo taken on 28th February, 2010, shown in Figure 5).

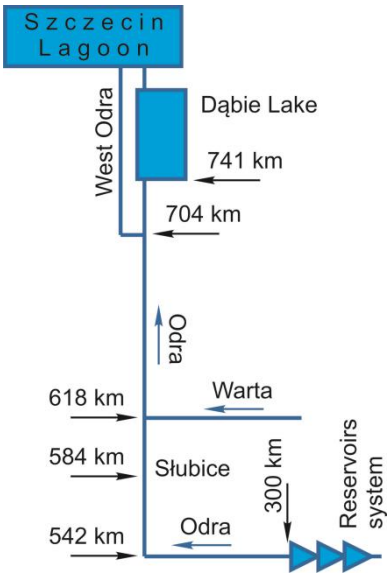

206

207 **Figure 4 Schematic view of the Middle and Lower Odra River (Note: figure out of scale)**

208

209 **Figure 5 Polish and German icebreakers escaping to the Warta River on 28th February, 2010 (railroad bridge at 615.1**
210 **river km) (RWMA, 2010)**

211 ### 1.2.2 Vistula river

212 The study covered the Vistula section between the existing Włocławek dam (674.75 river km) and the
213 planned Siarzewo dam (706.38 river km), covering a 31.6 km reach. In this section, ice processes are
214 affected by existence of the first locating dam and will be significantly changed due to new Siarzewo
215 project. The bathymetry of the model domain was described by 32 cross-sections surveyed by the
216 Institute of Meteorology and Water Resources in April 2018, reported by the National Water
217 Management Authority 'Wody Polskie' (NWMA). Topographic data were developed on the basis of a
218 digital elevation model obtained from the state of geodetic resources
219 https://pzgik.geoportal.gov.pl/imap; with a resolution of 1cm in vertical and horizontal direction.

In addition, the model domain includes the proposed elevation of the entrance area of the spillway (36.6 m above sea level) and the proposed entrance basin of the hydropower plant (35.5 m above sea level). Also, the left floodplain of the river bank located immediately upstream of the planned hydroelectric power plant requires dredging. It was assumed that the area would be dredged to a level of 36.6 m a.s.l. Bathymetric data together with topographic data used to build the mathematical model are shown in the Figure 6.

The existence of artificial islands has been taken into account in all simulations. A total number of 15 islands are designed, as part of an ecological compensation scheme, along both banks of the reservoir. The islands were proposed to provide habitat areas for birds (i.e. common tern, little ringed plover, kingfisher) nesting in the river shoals which will be flooded due to the creation of the reservoir. Thus, the islands are designed in the form of sandy areas exposed over the normal water level, and mildly sloping beaches. It was assumed that the shoreline of each island is at the normal pool level of the proposed reservoir (46.0 m a.s.l), and the central part of each island is flat and exposed by 1 m above the pool level (47.0 m a.s.l.). The shorelines, are shown in Figure 6b, while the bathymetry of the area, including the islands, is shown in Figure 6a.

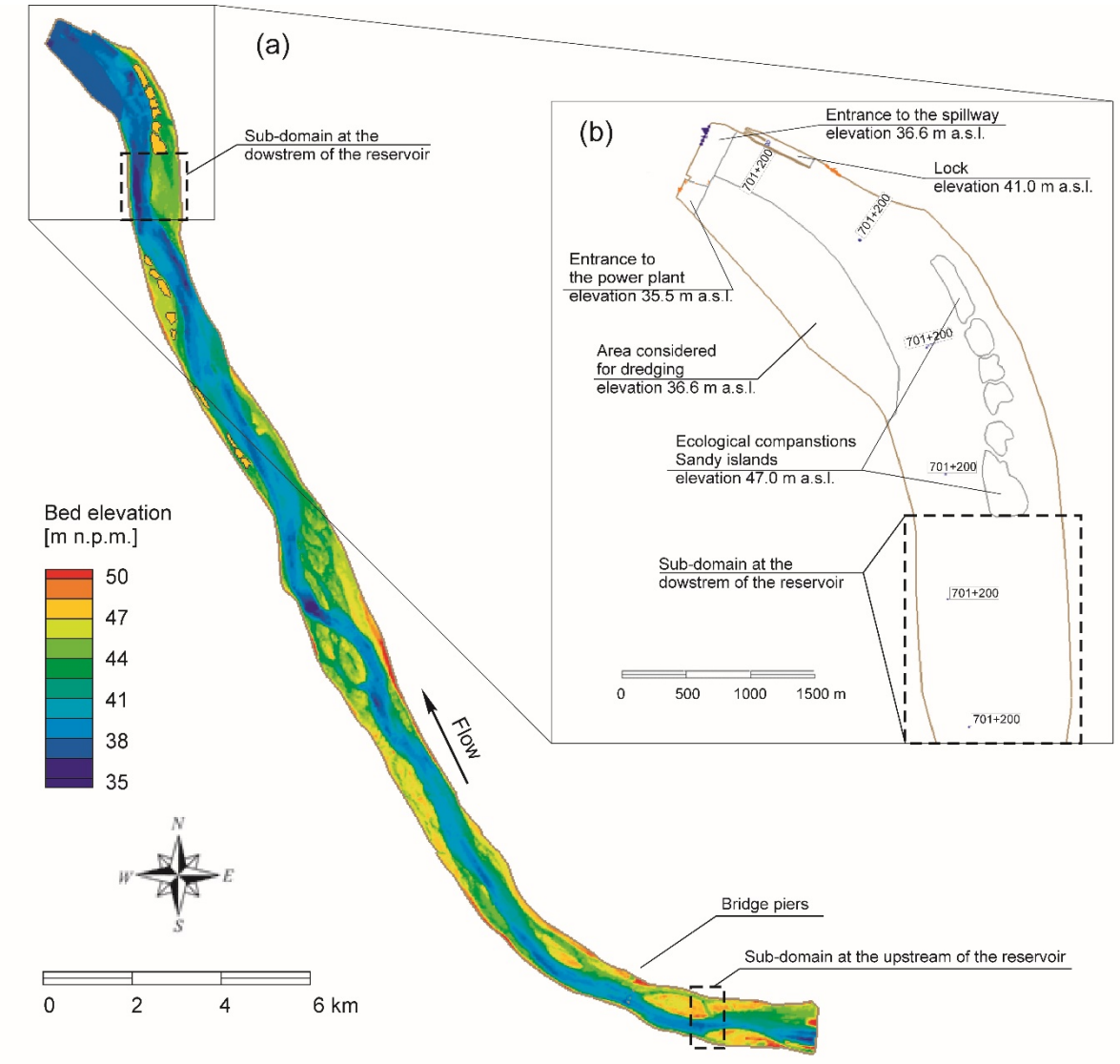

Figure 6 Siarzewo reservoir bathymetry included in the mathematical model showing islands and sub domain areas (a); downstream section of the model domain all the areas of modified bathymetry (b)

In the downstream section of the reservoir, the area adjacent to the Vistula left bank is a low-lying floodplain with riparian vegetation and wetlands which support a rich ecosystem. Due to the dam construction, the pool level in the reservoir will cause a floodplain area, which will be permanently inundated. Thus it is necessary to ensure that potentially deteriorated habitats are recreated by the planning of sandy islands to be built in the reservoir. The group of 6 islands is proposed close to the dam (about 3.5 km upstream) and, as shown by the numerical results, these islands significantly threaten the ice run.

In the upper section of the reservoir, about 4.5 km downstream from Włocławek dam, there is a bridge which deck is supported by 6 piers with semi-circular ends, 96.32 m apart from each other (Figure 7). All piers will be in the wetted area, once the pool level is achieved in the new reservoir. The bridge piers located within the route of the ice run will hamper its movement downstream, and could cause ice jamming (Szydlowski and Kolerski, 2018). Due to the significant impact of these bridge piers on the ice dynamics in the immediate vicinity of Włocławek dam, they were included in the model in the form of a closed land boundary, as shown in Figure 8.

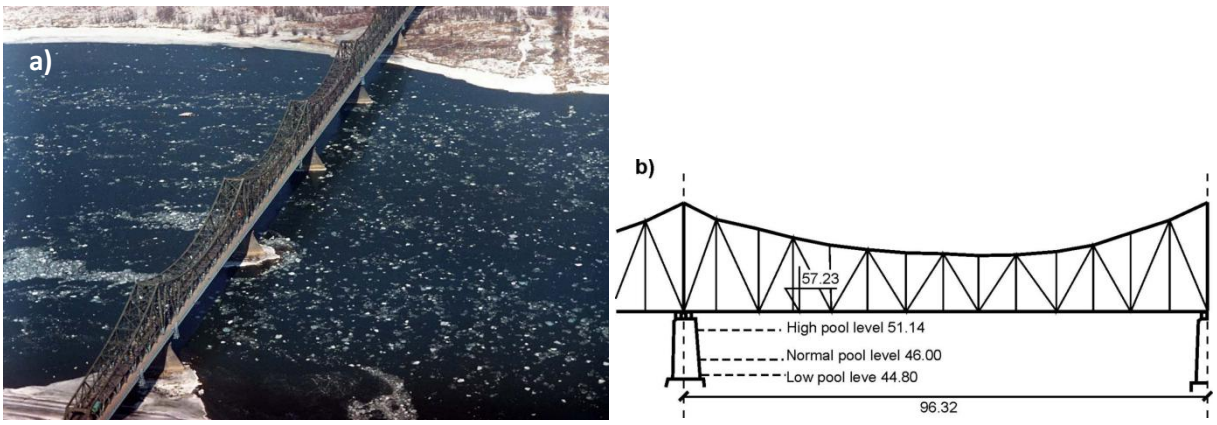

Figure 7 Frazil and pancake ice runs under the bridge in Wloclawek, photo courtesy of prof. Marek Grześ (a); a typical section of the bridge at 679+200 river km (b)

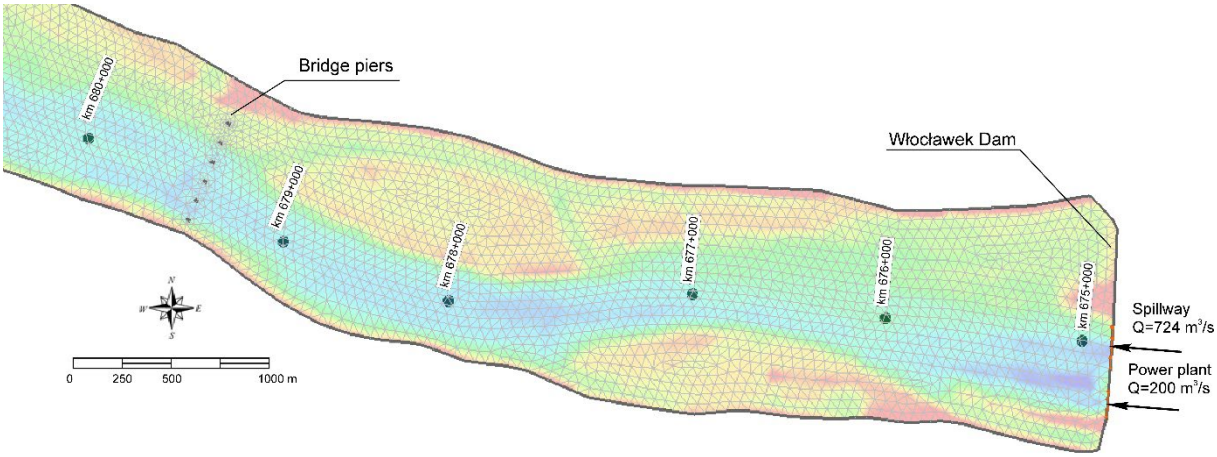

Figure 8 Upstream section of the model domain showing finite element mesh with bridge pier locations, river mileage and upstream boundary conditions for average flow Q_{ave} = 924 m³/s

1.3 Model description

The DynaRICE model allows the forecasting of both the place and time of an ice jam occurrence (Knack and Shen, 2018; Kolerski and Shen, 2015). The DynaRICE model is able to provide information on the

spatial and temporal distribution of ice in a river with a minimal user intervention limited to the task of the inputting data such as bathymetry, meteorological conditions and hydrodynamic data on the open boundaries of the domain (Carson et al., 2011). This means that the user does not need to know a priori location of the ice jam toe or the time of its formation. This is particularly important in the case of simulating processes resulting from planned structures(Knack and Shen, 2017). Then, objectively, only on the basis of the balance of forces and other external factors, can information on potential ice accumulation and jamming be obtained. In order to reduce computation effort, the modelling domain is limited to only areas where ice jams are expected to occur. The domain includes locations important from ice jamming processes point of view without expansion of the calculation time to a great extent. The model was set up to simulate the ice run in the typical flow expected at the beginning of the winter season and breakup conditions. The hydrodynamic module is based on the mass and momentum equations including mutual interaction between ice and water flow that are shown in conservation form (Shen et al., 1990):

$$\frac{\partial H_w}{\partial t}+\frac{\partial q_x}{\partial x}+\frac{\partial q_y}{\partial y}=\frac{\partial}{\partial t}\left(N\eta'\right), \qquad (1\text{-}1)$$

$$\frac{\partial q_x}{\partial t}+\frac{\partial}{\partial x}\left(\frac{{q_x}^2}{H_w}\right)+\frac{\partial}{\partial y}\left(\frac{q_x q_y}{H_w}\right)=\frac{1}{\rho}(\tau_{sx}-\tau_{dx})+\frac{1}{\rho_w}\left(\frac{\partial T_{xx}}{\partial x}+\frac{\partial T_{yx}}{\partial x}\right)-gH_w\frac{\partial h}{\partial x}, \qquad (1\text{-}2)$$

$$\frac{\partial q_y}{\partial t}+\frac{\partial}{\partial x}\left(\frac{{q_y}^2}{H_w}\right)+\frac{\partial}{\partial x}\left(\frac{q_x q_y}{H_w}\right)=\frac{1}{\rho}\left(\tau_{sy}-\tau_{dy}\right)+\frac{1}{\rho_w}\left(\frac{\partial T_{xy}}{\partial x}+\frac{\partial T_{yy}}{\partial x}\right)-gH_w\frac{\partial h}{\partial y}. \qquad (1\text{-}3)$$

In which $q_x$and q_y denote water discharge in x and y directions (the flow under the ice cover and seepage flow through the ice); h is water surface elevation [m]; η' indicates ice thickness from the underside surface to the water level [m]; τ_{sx} and $\tau_{sy}$are shear stresses on the water surface in x and y direction [Pa]. It either refers to the shear stress on the underside surface of the ice $\left(\tau_{ix,y}\right)$ or the water surface caused by the wind $\left(\tau_{ax,y}\right)$; $\tau_{dx}$and τ_{dy} are shear stress on the river bed in x and y direction [Pa]; N is ice concentration [−]; ρ_w is water density [kg·m^3]; H_w denotes total water depth underneath an equivalent ice-water interface $H_w/d_w=q/q_s$ [m]; d_w is water depth under the ice;

$q_s$is seepage discharge. T_{xy} is a turbulence tensor. Bed shear stress is calculated from (Shen et al., 1990):

$$\tau_{dx} = \frac{{n_d}^2}{(\alpha_d d_w)^{1/2}} \rho g \frac{q_x \left({q_x}^2 + {q_y}^2\right)^{1/2}}{{d_w}^2} , \quad (1\text{-}4)$$

$$\tau_{dx} = \frac{{n_d}^2}{(\alpha_d d_w)^{1/2}} \rho g \frac{q_y \left({q_x}^2 + {q_y}^2\right)^{1/2}}{{d_w}^2} . \quad (1\text{-}5)$$

Parameter α_d is the fraction of the water depth affected by the bed friction, $\alpha_d = A_d/A$; n_d is the Manning's roughness coefficient for river bed. On open water surface, the wind shear stress on water surface is calculated from (Shen, 2016):

$$\tau_{a,x} = C_w \rho_a {V_a}^2 \cos\xi_a , \quad (1\text{-}6)$$

$$\tau_{a,y} = C_w \rho_a {V_a}^2 \sin\xi_a . \quad (1\text{-}7)$$

In which ξ_a is the angle of wind vector (between wind direction and x axis); $C_w = 0.00155$, is wind drag coefficient (Wu, 1973); V_a is wind velocity; ρ_a is air density.

In the DynaRICE model the dynamic transport of the river ice is mathematically described as the movement of the number of particles carrying all ice properties and being subjected to the force balance. The governing equation for ice dynamics can be presented in the following form (Shen et al. 2000):

$$M_L \frac{d\vec{V}_L}{dt} = \vec{R} + \vec{F}_a + \vec{F}_w + \vec{G} \quad (1\text{-}8)$$

In which M_L is mass per area of parcel, $\vec{V}_L$ is ice velocity vector, $\frac{d\vec{V}_L}{dt}$ is surface ice acceleration, $\vec{R}$ is an ice internal resistance force, $\vec{F}_a$ is a wind drag force, $\vec{F}_w$ is a water drag force, $\vec{G}$ is gravitational force. In two dimensional coordinate system (depth averaged), internal ice resistance can be described in following way (Shen et al., 2000):

$$\vec{R} = \vec{\imath} R_x + \vec{\jmath} R_y , \quad (1\text{-}9)$$

$$R_x = \frac{\partial}{\partial x}(\sigma_{xx} N\eta) + \frac{\partial}{\partial y}(\sigma_{xy} N\eta)\,, \qquad (1\text{-}10)$$

$$R_y = \frac{\partial}{\partial x}(\sigma_{yx} N\eta) + \frac{\partial}{\partial y}(\sigma_{yy} N\eta)\,, \qquad (1\text{-}11)$$

In which, σ_{xx} and σ_{yy} are internal ice stresses in normal direction built up in ice rubble, $\sigma_{xy} = \sigma_{yx}$ are internal ice stresses in tangential direction. Internal stresses are calculated from viscoelastic–plastic constitutive model with Mohr-Coulomb yielding criterion for the ice as described in (Ji et al., 2005). Other terms from equation (1-8); .i.e. wind and water drag, as well as gravitational force can be calculated as follows:

$$\vec{F}_a = \vec{\imath}\left[\rho_a C_w \left|\vec{V}_L - \vec{W}\right|(u - W_x)N\right] + \vec{\jmath}\left[\rho_a C_w \left|\vec{V}_L - \vec{W}\right|(v - W_y)N\right] \qquad (1\text{-}12)$$

$$\vec{F}_w = \vec{\imath}\left[\rho \frac{{n_L}^2}{(\alpha_d d_w)^{1/2}}\left|\vec{V}_L - \vec{V}_w\right|(u - u_w)N\right] + \vec{\jmath}\left[\frac{{n_L}^2}{(\alpha_d d_w)^{1/2}}\left|\vec{V}_L - \vec{V}_w\right|(v - v_w)\,N\right] \qquad (1\text{-}13)$$

$$\vec{G} = -\vec{\imath} M_L g\left(\frac{\partial \eta}{\partial x}\right) - \vec{\jmath} M_L g\left(\frac{\partial \eta}{\partial y}\right) \qquad (1\text{-}14)$$

$\vec{V}_w = u_w\vec{\imath} + v_w\vec{\jmath}$ is water velocity vector, $\vec{V}_L = u\vec{\imath} + v\vec{\jmath}$ is surface ice velocity vector, $\vec{W} = \overrightarrow{W_x}\vec{\imath} + \overrightarrow{W_y}\vec{\jmath}$ is a wind velocity vector referred to the wind velocity on 10 m height above the water surface, n_L is ice roughness, d_w is a water depth under the ice[m]. The solution of the unsteady hydrodynamics is based on the Finite Element method (explicit upwind Galerkin scheme), and for the ice dynamics, the Smoothed Particle Hydrodynamic (SPH) method is used (Shen et al., 2000).

1.3.1 Model parameters description

The DynaRICE model has many parameters that must be determined or calibrated by the user. The most influential physical and numerical parameters are presented in Table 1. Considering the single layer ice and ice accumulation, the default values for the Manning's coefficients were used; however, to include local characteristics of the ice, the values varied for both sites. At Vistula River, the ice will be delivered from the reservoir located at the upstream open boundary. Thus, the ice entering the domain is the fragmented static ice cover from the reservoir, which its underside is smooth ($n_i = 0.02\ \mathrm{s}\cdot\mathrm{m}^{-1/3}$ was used). At the Odra River, the ice is mainly from the fragmented static ice cover,

originated from the system of reservoirs located at a longer distance (approximately 100 km) in comparison with Vistula River. Since the distance from the reservoir to the subjected area is long, possible frazil deposition could occur at the underside of ice floes. This is why the resistance for the single layer was increased from the default value to $n_i = 0.025\ \mathrm{s \cdot m^{-1/3}}$. The Manning's roughness coefficients for ice jam was set to be identical for both sites ($n_i = 0.06\ \mathrm{s \cdot m^{-1/3}}$). The initial ice thickness was used as 30 cm for both rivers based on the Institute of Meteorology and Water Management – National Research Institute (IMWM–NRI).

The group of parameters for Ice concentration were set to default values, which were set as 1.0 for static ice, 0.9 for surface frazil and 0.6 for ice rubble and floes accumulation. The value of the maximum concentration for ice rubble (0.6) is based on the assumption that ice jam has a porosity of 0.4 (Prowse, 1990). This value was calibrated by means of the physical model study (Tuthill et al., 2008, 2008) and data from the historical ice jams, .i.e., the Thames River (Kolerski et al., 2016) and the St John River (Knack and Shen, 2016).

The stoppage criteria is a model parameter, which is responsible for artificially stopping the ice. This situation happens if the ice moves slowly, possibly attaching to other ice pieces or the border ice. At the aim of not considering any artificial stoppage or subjectively controlled ice jamming, this parameter was set to zero.

Table 1. Calibrated parameters in the Odra and the Vistula Rivers. Parameters expected values available are referenced to literatures.

Parameter	Unit	Value calibrated for the Odra	Value calibrated for the Vistula	Reference literature (if applicable)
Manning's roughness coefficient for single layer ice	$[\mathrm{s \cdot m^{-1/3}}]$	0.025	0.02	(Ashton, 1986)
Manning's roughness coefficient for ice jam	$[\mathrm{s \cdot m^{-1/3}}]$	0.06	0.06	(Ashton, 1986)
Initial ice thickens	[m]	0.3	0.3	
Ice internal friction angle	[°]	46	46	(Lal and Shen, 1991)

Wind-ice stress coefficient	$[-]$	0.0015	0.0015	(Wu, 1973)
Maximum concentration of ice parcels in jam	$[-]$	0.6	0.6	(Prowse, 1990)
Maximum concentration for skim ice and border ice formation	$[-]$	1.0	1.0	(Lal and Shen, 1991; Timalsina et al., 2013)
Maximum concentration for frazil ice	$[-]$	0.9	0.9	(Schneck et al., 2019)
Stoppage criteria for ice	$[\mathrm{m} \cdot \mathrm{s}^{-1}]$	0	0	
Total number of nodes in the domain	$[-]$	11311	22598	
Initial parcel size (for SPH calculation)	[m]	25	30	

333

334 ### 1.3.2 Boundary conditions

335 #### 1.3.2.1 Odra river

336 Boundary conditions related to river hydrodynamic were set to represent the flow conditions
337 observed during winter months. The data from Słubice gauging station were analyzed, where the
338 daily water surface elevation is recorded. The water discharge is also provided for the Słubice station.
339 In addition, the station has some ice thickness observations; however, this is mostly qualitative
340 information on the ice type (Wolski et al., 2017; Marszelewski and Pawłowski, 2019). Since detailed
341 ice conditions for the Lower Odra River are not known, the input data for the model were set at the
342 upstream boundary for an initial ice floe thickness of 0.3 m. The calculations do not include any
343 border ice, nor do they consider existing ice cover in the river. Thus, it was assumed that the river is
344 free of ice, and is subjected to possible ice jamming from breakup ice transported from upstream.

345 The data from 11 years of water discharge recorded at Słubice gauging station were analyzed to
346 estimate flow conditions for modeling. Data were provided by the hydrologic surveillance service of
347 the Institute of Meteorology and Water Management – National Research Institute (IMWM–NRI).
348 Also, for the current study, the data were retrieved from < https://dane.imgw.pl/ >. In Poland, the
349 water year is used for hydrological statistics; thus, the time series starts on 1st November, 2006 and
350 ending on 31st October, 2017 was used for the study. The more recent data was not available at the

time of conducting the study. The raw flow data is presented in Figure 9, and the discharge - time duration plot for an average year in Figure 10. The winter season was indicated in Figure 9 by marking the time with blue color (1st December – 31st March) .

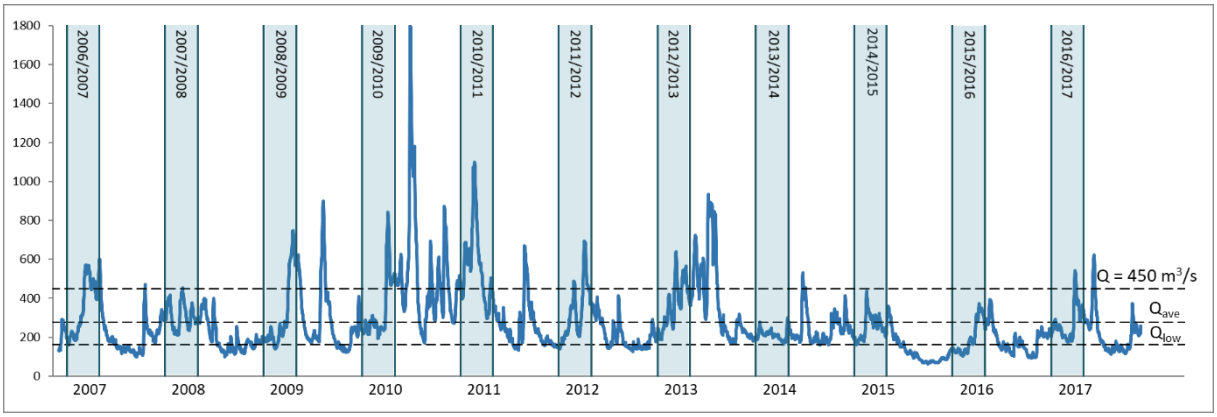

Figure 9 Water discharge at Słubice gauging station; winter seasons were marked with blue, and characteristic flows designated by dashed lines (data from https://dane.imgw.pl/)

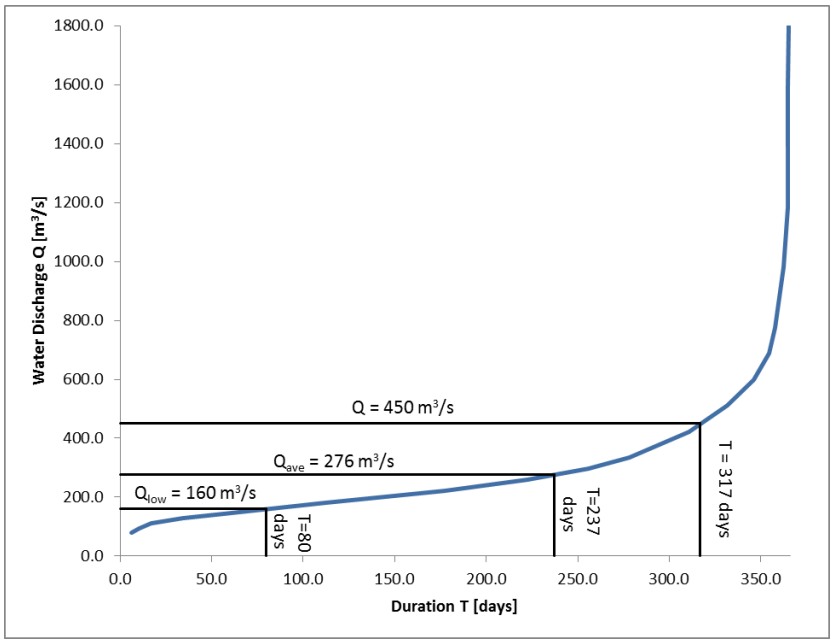

Figure 10 Water discharge duration for an average year at Słubice gauging station; flows used in the study and their durations were marked with black lines (data from https://dane.imgw.pl/)

The study considered three water discharge conditions: namely, yearly-average flow by Q_{ave} = 276 m^3/s (based on the 10-year daily average data), low flow by Q_{low} = 160 m^3/s, and flow referring to the breakup condition Q = 450 m^3/s. Typically for the beginning of the winter season, the flow in the Odra River is reduced below the average flow, however rarely dropping to the low flow range. In

recent years, the only exception was the 2015/16 season, which was affected by extreme drought in the summer season (Staśko and Buczyński, 2018). In consequence, during the entire winter season, low water levels and discharge were observed.

The so-called 'typical breakup conditions' for Słubice (Q = 450 m^3/s) refers to the average flow from March. It is also the flow recorded on 27th February, 2010 during the mid-winter breakup, when the case of an ice jam in Słubice developed due to the ice sluicing. In many years, in the second half of the winter, the water discharge rose due to increased air temperature and melting snow, as well as ice breakup. Recently, an increased discharge is more common for mid-winter, which is caused by the changing long-term state of the atmosphere in the region. As a result, a mid-winter breakup may occur leading to a potential ice jamming. Due to the frequency occurrence of the mentioned circumstances, they were included in the simulations.

1.3.2.2 Vistula river

The upstream open boundary conditions were set at the cross-section of the existing Włocławek diversion dam, in such a way that the dominant part of the flow was conveyed through the spillway, and the rest through the power plant. The flow distribution was set according to the operation procedure during ice sluicing, which is published yearly by RWMA Warszawa (RWMA, 2009). At the downstream end of the model located at the proposed Siarzewo dam, the constant water surface elevation was set up according to the proposed normal pool level. In addition, the outflow boundaries were set at the proposed hydropower plant and the bypass channel. The downstream open boundaries for water were assumed in the nodes located in each spillway section, at the turbine outlets and the bypass channel (fish passage inlet). It was considered for setting the ice boundary condition that ice sluices solely through the spillway.

The following calculation conditional variants, from the hydrodynamics point of view, were carried out for the numerical analysis: average flow Q_{ave} = 924 m^3/s and discharge of 1308, 3008, 4538 and 6104 m^3/s. As an example, the boundary conditions for water discharge Q = 924 m^3/s are shown in

figure 8 and 11. At the upstream flow boundary, the proportions were set as 724 m^3/s in the spillway and 200 m^3/s in the power plant (see Figure 8). At the model downstream, both the water surface elevation and discharge conditions were used. Water discharge was set at two locations: the inlets to the power plant and the entrance to the bypass channel, while the water surface elevation conditions were used at the spillway. The constant water level of H = 46 m a.s.l. was used, which is the equivalent of the normal pool level at the proposed reservoir. Water discharge was set up for the value of 200 m^3/s through the hydropower plant (carried out through one of seven turbines, no 4, counted from the left bank). In addition, the water flow of 20 m^3/s was conveyed through the bypass channel. The remaining part was distributed over 5 out of 15 spans of the spillway, but no specific value for the discharge was used due to the WSE boundary conditions applied at the spillway. Three spillway opening setups were tested (as shown in Figure 11), assuming the spans in the immediate vicinity of the power plant (span no 1) and the lock (no 15) always being closed.

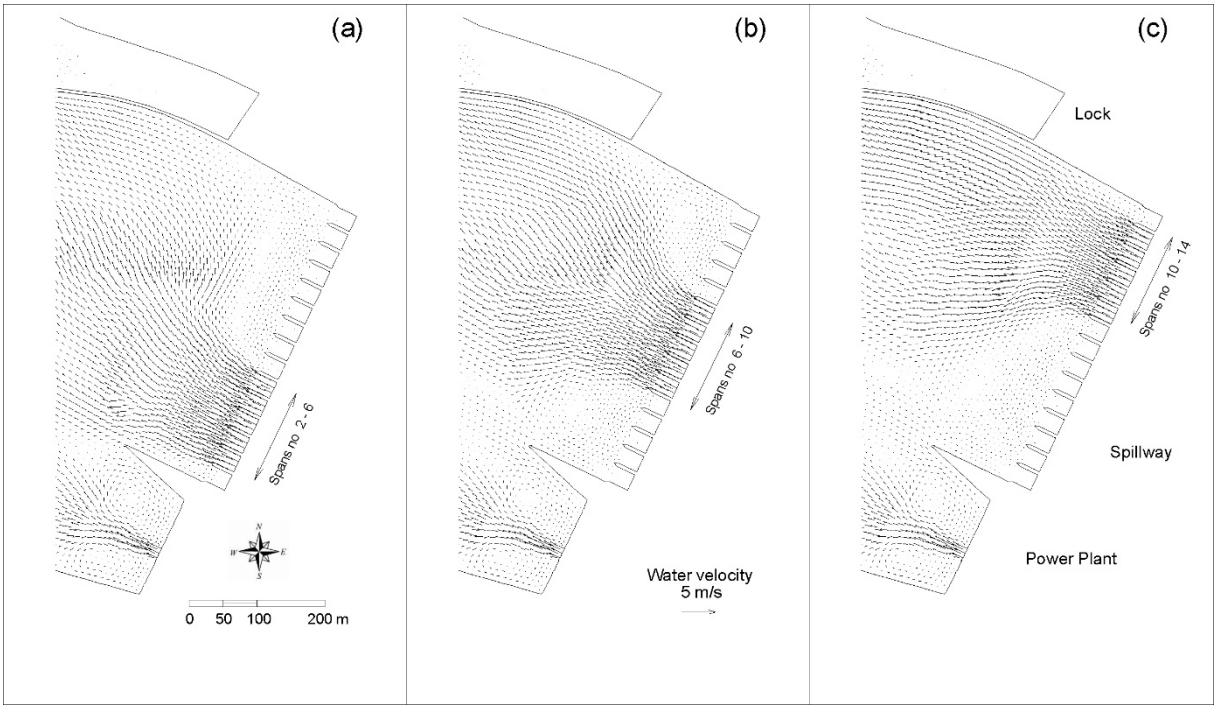

Figure 11 Siarzewo spillway opening systems used for calculations at a flow of 924 m^3/s, open spans from 2 to 6 (a), open spans from 6 to 10 (b) and open spans from 10 to 14 (c); Note, the river section shown in the figures is downstream of the proposed dam and is not included in the current simulations

All numerical simulations were carried out with and without taking into account the wind action. For those cases applied under the wind effect influence, the wind blows from the west, north, east and south with a speed of 3 m/s for average flow conditions, and 4 m/s for all other simulated cases. The reduced wind speed for average water flow was based on the fact that the ice was not able to run downstream of the reservoir, drifting towards the banks (for the wind velocity of 4 m/s).

Table 2. Scenarios proceeded for the Vistula River study

Case no	Water discharge	Spillway opening spans from left	Wind	
			Speed	Direction
[-]	m^3/s	[-]	[m/s]	[-]
1	Q = 924 m^3/s	0xxxxx000000000*	0	No wind
2			3	W ⇒
3			3	S ⇑
4			3	E ⇐
5			3	N ⇓
6		000000000xxxxx0	0	No wind
7			3	W ⇒
8			3	S ⇑
9			3	E ⇐
10			3	N ⇓
11		00000xxxxx00000	0	No wind
12			3	W ⇒
13			3	S ⇑
14			3	E ⇐
15			3	N ⇓
16	Q = 1308 m^3/s	0xxxxxxxx000000	0	No wind
17			4	W ⇒
18			4	S ⇑
19			4	E ⇐
20			4	N ⇓
21		000000xxxxxxxx0	0	No wind
22			4	W ⇒
23			4	S ⇑
24			4	E ⇐
25			4	N ⇓
26	Q=3008 m^3/s	0xxxxxxxxxx0000	0	No wind
27			4	W ⇒
28			4	S ⇑
29			4	E ⇐
30			4	N ⇓
31		0000xxxxxxxxx0	0	No wind
32			4	W ⇒
33			4	S ⇑
34			4	E ⇐
35			4	N ⇓
36	Q = 4538 m^3/s	0xxxxxxxxxxxx0	0	No wind
37			4	W ⇒
38			4	S ⇑
39			4	E ⇐

40			4	N ⇓
41	Q = 6104 m^3/s	0xxxxxxxxxxxx0	0	No wind
42			4	W ⇒
43			4	S ⇑
44			4	E ⇐
45			4	N ⇓

*) 0 – closed; x – open

In total, 45 number of simulations were made. The initial ice thickness was established at 0.3 m and the ice was discharged through a spillway with an initial concentration of 0.4 for all analyzed cases. This means that at the upstream boundary conditions, a 0.3 m thick ice inflow with a surface concentration of 0.4 was implemented over the entire time of the simulation. It should be noted that the maximum permissible ice jam concentration in the DynaRICE model is 0.6, and a further increase in the concentration leads to an increase in jam thickness. Due to the protection of the inlet to the hydroelectric power plant against incoming ice, in all simulations, it was assumed that the ice cover remained intact on the right bank of the reservoir for a distance of about 2 km upstream of the dam, overlapping with the dredged area shown in Figure 6.

1.4 Methodology

The process of locally reduced conveyance of ice transport resultant from channel narrowness, in the case of a continuous ice inflow from upstream, often initiates an ice jam. Over time, it will lead to an increase in the ice thickness and a constriction of the river cross-section, which results in the impeded water outflow and an increase in water surface elevation in the section upstream of the jam. This process is well known and described in the literature (Beltaos, 1995; Shen et al., 2008; Pawłowski, 2019) as a phenomenon responsible for ice jam processes on rivers. For the estimation of the congestion potential of a selected location on a river, both the following factors, ice velocity and ice thickness change in time; thereby must be taken into account as indicators. This method for the estimation of the jam potential was used in the past (i.e. (Knack and Shen, 2017; Shen et al., 2005)); however, for the purpose of this study, a modified procedure was proposed. The current method is taking into account the change in the ice velocity in relation to the water velocity, and the increase in the ice thickness in relation to the initial thickness of a single ice floe. This criteria is only applicable

for the break-up ice jam conditions without considering the thermal effect on the ice run. Thermal processes could change proposed thresholds.

Four criteria for assessing ice jamming were adopted: (0) no jam, (1) jam possible, (2) jam probable, (3) ice jam. No ice jam implies that ice is proceeding without stop, and neither increased thickness nor reduction of the ice velocity is projected. Jam conditions (1) and (2) refer to some reduction in the ice velocity, as well as an increase in the surface ice concentration. The possible jam condition (1) indicates increased ice concentration due to a reduction in ice velocity, leading to some thickening of ice. Using the above criterion, an analysis of the jam potential of the two Polish rivers was carried out: the Vistula River, at the upstream of the planned Siarzewo diversion dam, and the Odra River in the Słubice region after the modernization of the river training structures. All threshold conditions are summarized in Table 3.

Table 3. Conditions used in the study to determine the jam potential for the numerical model results

Jam potential	$\frac{\text{Ice velocity } (V_i)}{\text{Water velociy } (V_w)}$	$\frac{\text{Ice thickness } (\eta_i)}{\text{Single floe thickness } (\eta_0)}$
(0) No jam	>0.9	<1.1
(1) Jam possible	0.9 – 0.5	1.1 – 2.0
(2) Jam probable	0.5 – 0.15	2.0 – 3.0
(3) Ice jam	< 0.15	> 3.0

Once the calibrated mathematical model is implemented in the selected areas, the numerical simulations can be processed, and the obtained results must be analyzed in terms of ice accumulation and jamming.

2 Results and discussion

2.1 Odra River

To check the ice conditions in the vicinity of the Słubice-Frankfurt Bridge, a mathematical model was applied to a 5 km longitudinal section of the Odra River. Probable ice jam conditions represent the case in which the increased ice thickness is more than 2 times the initial ice thickness. Also, in this case, the area-averaged ice velocity in an initially specified location drops below 50% of the average water velocity in that area. Ice jam conditions are defined by a further velocity reduction to 15% of the water velocity, and the ice thickness increasing to 3 times the initial, single ice floe thickness.

The results showed a consistent trend over the time; although, the results from the last hour are discussed in this study. For the low flow, ice transport through the bridge cross-section is hampered and the ice accumulation is observed. A comparison of the ice thickness distribution for high ice inflow ($Q_i/Q_w = 0.048$) is presented in Figure 12 in the form of a contour plot of the 24th hour of simulation. It shows increased ice thickness upstream of the bridge cross-section. The cause of such a formation is ice congestion since the ice transport is severely hindered by the reduced cross-section. In this hydrodynamic condition, the reconstructed river training structures affected the ice transport insignificantly.

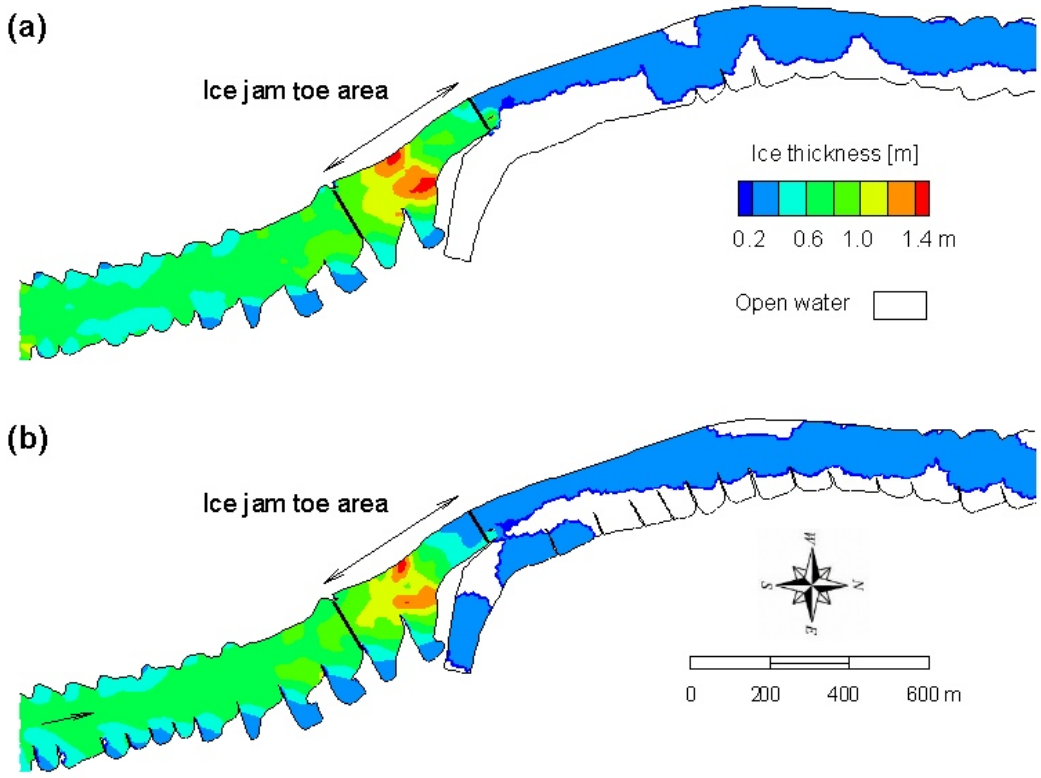

466

467 **Figure 12 Simulation results of ice thickness at low flow ($Q_w = 160\ m^3/s$) and high ice inflow ($Q_i/Q_w = 0.045$) for**
468 **current (a) and proposed (b) conditions; sub-domain for numerical jam analysis designated by black lines**

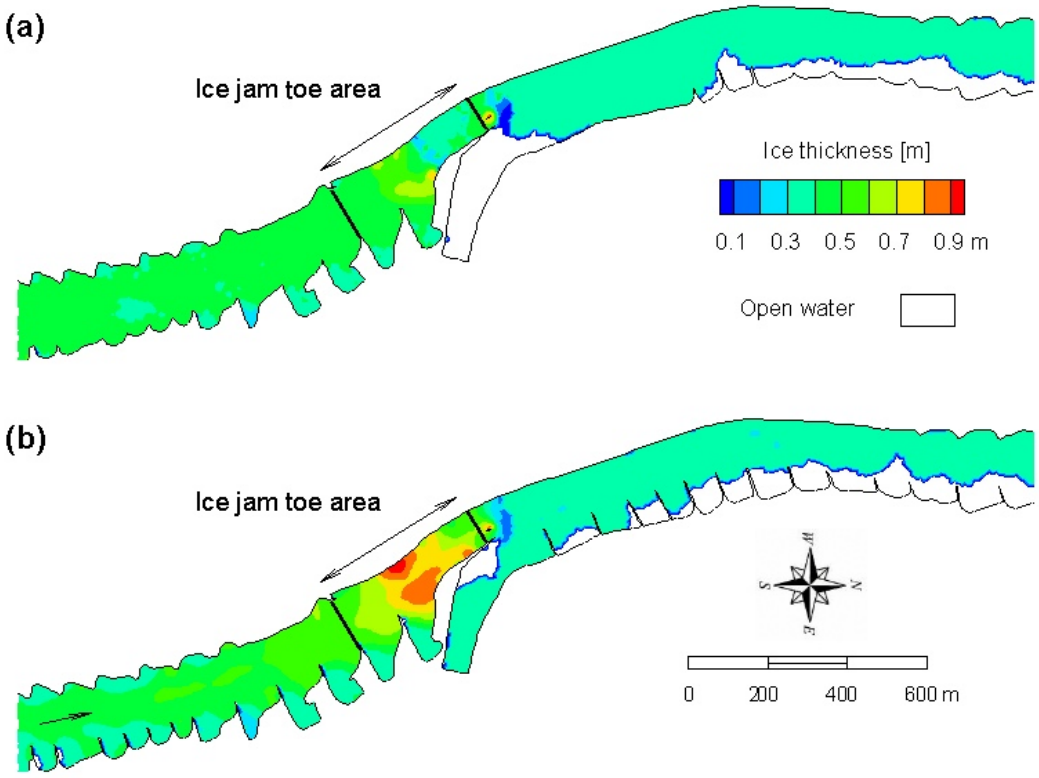

Figure 13. Simulation results of ice thickness at average flow ($Q_w = 276\ m^3/s$) and high ice inflow ($Q_i/Q_w = 0.048$) for current (a) and proposed (b) conditions; sub-domain for numerical jam analysis designated by black lines

The results for average flow showed , the proposed structures reduced the river capacity for ice transport. Since the constant ice concentration is applied as the upstream boundary condition, different magnitude of water discharge changes the amount of the ice inflow and the resulting ice volume in the domain. Three cases of different ice inflow were simulated and all the calculation results with the proposed structures led to a larger ice accumulation in comparison to the current conditions. The final results of the case with average flow (Q_w = 276 m^3/s) and high ice discharge ($Q_i/Q_w = 0.048$) are shown in Figure 13.

All simulation results with high water discharge (Q_w = 450 m^3/s) showed that ice is transported downstream, without stoppage. Only, is some insignificant shore accumulations perceptible for both the current and proposed regulating structures. Thus, the ice thickness distribution over the model domain is not presented in this domain. It is mainly caused by the low ice-to-water discharge ratio,

and high drag force from the increased water velocity. Consequently, ice is less prone to a stop and the release of any form of the accumulation would be facilitated by the high water drag force.

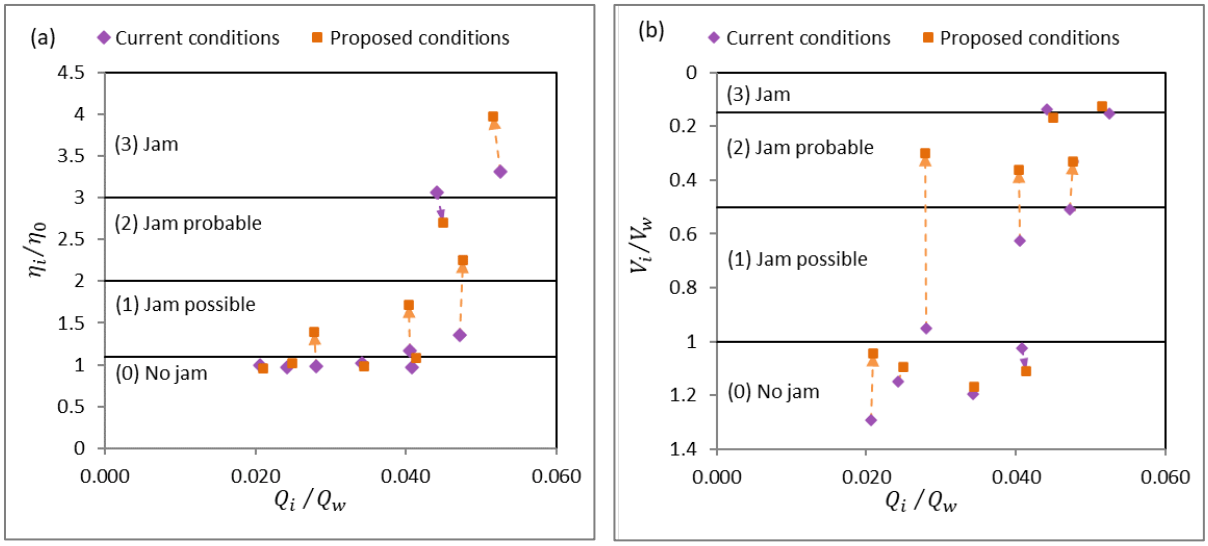

Figure 14 Numerical simulation results of ice jamming for the Słubice according to ice thickness increase **(a)** and ice velocity reduction criterion **(b)**; purple and orange clusters refer to current and proposed conditions, respectively

The simulation results are summarized in Figure 14 and Table 4, showing the ice jam potential for the aforementioned location. The analysis includes a wide variation of water and ice discharge, covering the conditions typical for winter months which are low or average flow. It also includes the condition which is common for breakup condition, and represented by flow above average with increased ice discharge. The numerical model results show, for most cases the ice run is hampered by new structures. The extension of the spurs will act towards a flow constriction and velocity increase in the main channel. However, in the vicinity of the bridge, the cross-section will be reduced by the newly designed structures. As a consequence, the congestion of the ice is observed due to the convergence of the flow. In addition, at the upstream of the river, the regulation increase the ice supply to the ice congestion area.

The influence of river regulation is particularly visible for the case of low water discharge (Q_w = 160 m^3/s and low ice inflow of $Q_i/Q_w = 0.028$). In such case, the new structures put a stop to the ice run. Simulation results show the reduction of the ice velocity to not more than 30% of the water velocity. However, due to the low flow in line with low water velocities, this case did not show a

significant increase in the thickness of the ice ($\eta_i/\eta_0 = 1.39$). It can be concluded that, from the two mentioned criterion, the velocity ratio is more likely to predict jamming. Since this study mostly concerns the low flow condition, in the case of ice blockage, water velocity is not high enough to develop thick ice jam toe. As a result, ice stoppage is more commonly evident than the increase of the ice thickness.

Table 4. Numerical simulation results for the Odra river, Słubice station

Model input; upstream boundary			Model results averaged over the sub-domain					Conditions
Water Discharge Q_w	Ice discharge Q_w	$\frac{Q_i}{Q_w}$	Ice thickness η_i	Ice velocity V_i	Water velocity V_w	$\frac{\eta_i}{\eta_0}$	$\frac{V_i}{V_w}$	
[m³/s]	[m³/s]	[m³/s]	[m]	[m/s]	[m/s]	[-]	[-]	C/P*
160	4.5	0.028	0.30	0.57	0.60	0.99	0.95	C
	4.5	0.028	0.42	0.17	0.55	1.39	0.30	P
	7.1	0.044	0.92	0.09	0.69	3.06	0.14	C
	7.2	0.045	0.81	0.10	0.60	2.70	0.17	P
	8.4	0.053	0.99	0.11	0.71	3.31	0.15	C
	8.2	0.052	1.19	0.08	0.68	3.97	0.13	P
276	11.2	0.041	0.35	0.60	0.96	1.17	0.62	C
	11.1	0.040	0.52	0.32	0.89	1.72	0.36	P
	6.7	0.024	0.29	1.08	0.94	0.97	1.15	C
	6.9	0.025	0.31	0.94	0.85	1.02	1.10	P
	13.0	0.047	0.41	0.49	0.96	1.36	0.51	C
	13.1	0.048	0.68	0.30	0.91	2.26	0.33	P
450	15.4	0.034	0.31	1.66	1.39	1.02	1.20	C
	15.5	0.034	0.29	1.47	1.26	0.98	1.17	P
	9.3	0.021	0.30	1.68	1.30	1.00	1.29	C
	9.4	0.021	0.29	1.29	1.24	0.96	1.04	P
	18.4	0.041	0.29	1.46	1.42	0.96	1.03	C
	18.6	0.041	0.33	1.37	1.23	1.09	1.11	P

*C – current conditions; P – proposed conditions

The simulation result indicates, although, spur dikes can increase the ice jam potential, they regulate the river by producing backwater effect. Because of the reduction in the cross section width, the water level increases. Since the increased depth can be considered as an advantage for the ice breakers to not be stuck in the shallow areas, mechanical ice breaking (with the advantage of ice breakers) is the proper approach in this circumstance. Therefore, both river regulation and increase in the water level provided by presented spur dikes will mitigate the ice jam related condition.

2.2 Vistula River

According to the obtained numerical model results, two areas of potential ice jamming were selected in the reservoir: the bridge cross-section and the downstream area where the proposed islands are designed. Both areas, as indicated in Figure 6, were considered for further analysis within the proposed methodology. The results are presented in Table 5 (upstream location) and Table 6 (location in the vicinity of the dam) for selected cases.

In the first mentioned location, which is a short distance downstream of the existing dam (679+200 river km, about 4.5 km), the piers of the bridge hinder the ice run. This is particularly likely in the event of low water flow and high ice concentration. Ice sluicing through the proposed dam shall not be performed if the water discharge does not reach the average flow conditions; therefore, low flow scenarios were not performed. Among all the calculated cases, the greatest risk of ice jamming is observed for simulations with average flow (Q_{ave} = 924 m^3/s), and wind blowing from the opposite direction to the water flow.

Under these conditions, the bridge opening (horizontal distance between two piers) is not sufficient to allow a continuous run of ice of high concentration. This leads to ice congestion and stop near the bridge piers in the central part of the river, which retards the ice movement, and in some locations, the formation and progression of the juxtaposed ice cover in an upstream direction. The process becomes more dynamic once the ice cover progression reaches the vicinity of 677 river km. In that section, the river originally meandered between alluvial islands on both banks; even though, due to the formation of the reservoir, the islands were inundated forming shoals hindering the ice run. It led to additional stops, and accelerated the accumulation of inflowing ice and eventual jam formation. For average flow conditions, ice was sluiced through 5 out of 15 spillway spans, and three configurations of spillway opening were tested. However, this has no effect on the ice dynamic in the upstream section of the reservoir.

Some effects were also observed for the discharge Q = 1308 m^3/s; however, in this case, it was only a local retardation of the ice movement and a negligible increase in the ice thickness at the upstream face of the bridge piers. While continuing the simulation, the process did not develop nor progress towards the upstream with time. For cases with a higher flow discharge, the water drag was sufficient to release any ice stop at the bridge cross-section and ice transport proceeded smoothly towards the downstream. Thus only cases with average discharge were considered for further testing within the proposed procedure. All simulation results are presented in Table 5 and also presented in a form of contour plot of the ice thickness in Figure 15.

The second location where ice jamming was observed is the area close to the proposed dam (701 - 703 river km).The calculations carried out for the average flow and a flow of 1308 m^3/s clearly show that, the locations of the mentioned artificial islands should be reconsidered, and the change in the layout of the southernmost island of the group is absolutely necessary. The southern front of the southern island (around 702+650 river km) is a place wherein due to the event of a wind blowing from the north and west, ice accumulation and potential ice jamming can occur. A change in the shape of the southern shore of the island should be considered to direct ice towards the spillway. For the higher flow velocity conditions, the water drag is high enough to push ice towards the spillway without any significant ice stop. Also, for the higher discharges, the ice flows in the shallow channel between the islands and the bank. The results of numerical modeling also indicated a significant force, exceeding 2 kN/m^2, to be transferred from the ice to the shore of the artificial islands. This force must be withstood by the islands' borders; although, considering the purpose of the islands, neither riprap nor concrete could be used to reinforce the shores.

Table 5. Simulation cases and obtained results for the Vistula River study for the water discharge Q = 924 m^3/s and single floe thickness η_0 = 0.3 m; area at the upstream of the reservoir (677 – 678 river km)

Case no	Water Discharge	Ice discharge	Spillway opening spans from left	Wind		Ice thickness (η_L)	Average velocity		$\frac{(V_i)}{(V_w)}$	$\frac{(\eta_i)}{(\eta_0)}$
				speed	direction		Ice (V_i)	Water (V_w)		
	[m^3/s]	[m^3/s]	[-]	[m/s]	[-]	[m]	[m/s]	[m/s]	[-]	[-]
39		12.3	00000xxxxx00000*	3	No wind	0.41	0.072	0.246	0.29	1.36

40		12.2		3	W ⇒	0.47	0.068	0.236	0.29	1.58
41		12.1		3	S ⇑	0.399	0.060	0.244	0.25	1.33
42	Q = 924	12.2		3	E ⇐	0.44	0.078	0.247	0.32	1.48
43	m^3/s	12.2		3	N ⇓	0.47	0.069	0.243	0.28	1.57

*) 0 – closed; x – open

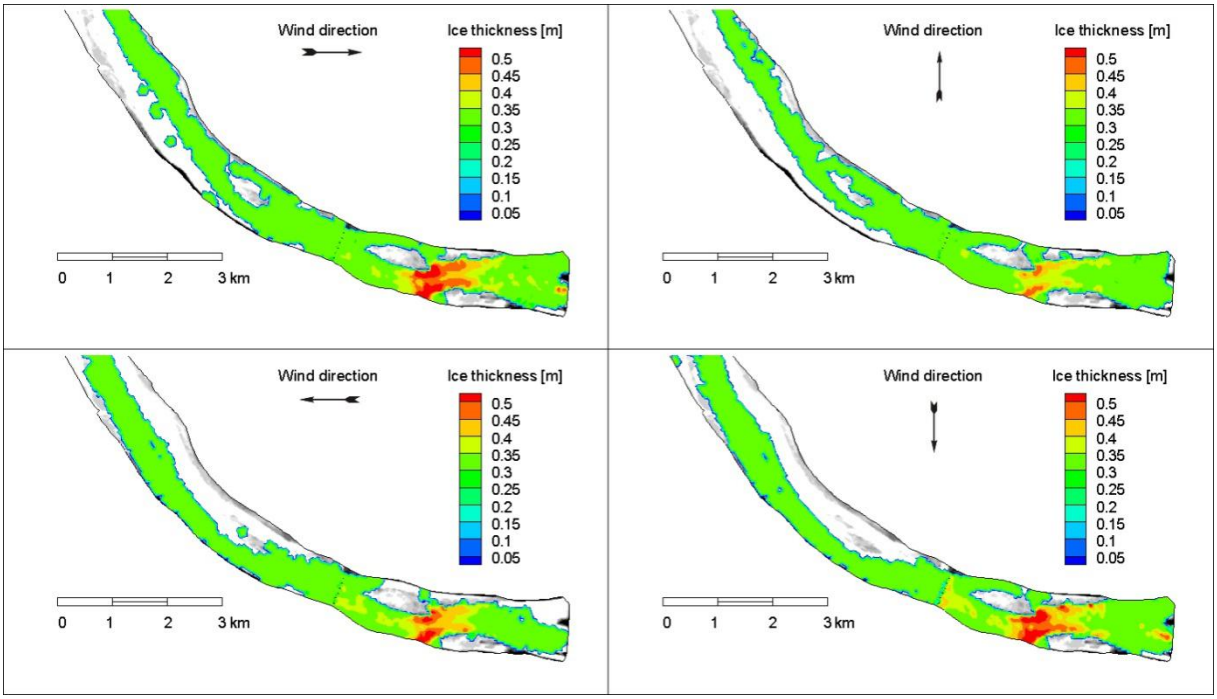

Figure 15 Ice thickness distribution in the upstream part of the proposed reservoir for the average discharge Q_{ave} = 924 m^3/s and varying wind direction at a speed of 3 m/s

Recently, before the new dam construction, some ice stops has been observed upstream of the bridge, as a result of ice sluicing from Włocławek spillway. The inflow to the new reservoir considers to be the outflow from the existing reservoir, which forms the upstream open boundary for the current model. Concerning the procedure of the icebreaking operation on Włocławek reservoir, the competent Water Authority should allow ice sluicing only if ice jamming on the reservoir is observed, or if a significant amount of ice is released in the river upstream of the reservoir. If the above-mentioned conditions occur, it is still not recommended to release ice for a water discharge below 1308 m^3/s. Thus, simulated cases with average water flow should be considered as worst-case scenarios, occurring only in very unusual conditions.

575 The simulation results indicate the strong effect of the river bathymetry on the ice transport,
576 compounded by the presence of the bridge piers and wind. At first, the ice cover develops upstream
577 of the bridge piers. During the time, the progressing ice cover in addition to the restriction at the
578 cross sections out of the existing islands, lead to an increase in the ice jam formation upstream of the
579 piers. That is mainly due to the fact that, at the restricted area between the islands, the water
580 velocity is increased (thereby, drag force of water rises), causing higher velocity for the ice run.
581 Entering the ice stoppage area, the ice particles become a part of the ice jam due to the ice
582 resistance force. As shown in Figure 15, all cases with average flow, where the two islands are
583 located and river meanders, show ice accumulation on both banks . After the reservoir is formed, the
584 water level will increase to the normal pool level. However, the most parts of the upstream section
585 of the proposed reservoir will preserve their river-like character, and the main currents will follow
586 the thalweg. According to the numerical results shown in Table 5, all cases with average flow will
587 cause a reduction in the ice velocity in comparison to the water velocity by more than 70%, except
588 for the case with an eastern wind. In this case, the wind accelerates the ice movement; although, due
589 to the existence of the bridge piers, ice flow converges and ice transport becomes limited, leading to
590 the ice accumulation in the upstream. Considering ice-to-water velocity conditions, all cases with
591 average flow represent a strong possibility of ice jam formation.

592 The increase in the ice thickness is variable from case to case, and in all five simulated cases, the
593 most severe conditions are expected for the case with the western and northern wind. In both
594 mentioned cases, wind pushes the ice in an oposit direction to the flow or towards the outer bank.
595 This causes additional resistance to the ice due to the contact between the ice and the banks. In
596 consequence, the ice increases in thickness by roughly 60 %, being classified as ‘ice jam probable’
597 type in both cases. Other cases similarly indicate increased ice thickness; although this growth
598 appears to be to a lesser extent, thusly being classified as ‘ice jam possible’ type.

The second area where ice jam potential was tested is within a distance of 4 km in the upstream direction from the proposed dam (703 – 704 river km, see Figure 6). In this location, the water surface elevation is nearly horizontal due to the backwater effect, and the water velocity is relatively low (based on the high water depth). With regard to the force balance on movable ice, the drag force from water is not significant, hence the impact of additional obstacles on the ice run in this area may cause ice stop. The ice movement is affected by the artificial islands located along the outer bank of the reservoir, which causes a narrowness of the cross-section area by about 12%. The upstream shore of the southernmost island was designed in a non-streamlined shape, which significantly impedes the both ice and water flow.

Ice jamming in the downstream section of the reservoir is less located. However, due to the proximity of the dam, as well as the wind and flow impact on the ice dynamic, the effect of the spillway opening was considered. The ice jam potential upstream of the dam was determined for above average water discharge (Q = 1308 m^3/s), with variable number of open spillway's spans and wind directions. For these hydrodynamic conditions, ice was supplied in the upstream of the model, with the surface ice concentration of N = 0.4. This value of concentration leads to the ice discharge varying from 13.3 m^3/s to nearly 15 m^3/s which is about 1% of the water discharge. Since the jam has no clear location of the toe, the averaged ice thickness was applied over the reach of about 2 km of the reservoir, upstream of the artificial islands. The same area was used at the aim of averaging out ice and water velocities, and all the results are summarized in the Table 6. The last two columns of the table are the relative ice-to-water velocity ratio and the increase in the ice cover thickness.

Table 6. Simulated cases and obtained results for the Vistula River study with the water discharge of Q = 1308 m^3/s and the single floe thickness η_0 = 0.3 m; area at the downstream of the reservoir (703 – 704 river km)

Case no	Water Discharge	Ice discharge	Spillway opening spans from left	Wind		Ice thickness (η_L)	Average velocity		$\frac{(V_i)}{(V_w)}$	$\frac{(\eta_i)}{(\eta_0)}$
				speed	direction		Ice (V_i)	Water (V_w)		
	[m^3/s]	[m^3/s]	[-]	[m/s]	[-]	[m]	[m/s]	[m/s]	[-]	[-]
1	Q = 1308	13.4	0xxxxxxx000000*	0	No wind	0.30	0.198	0.198	1.00	1.00
2		13.4		4	W ⇒	0.37	0.023	0.169	0.13	1.23

3		13.3		4	S ⇑	0.30	0.286	0.189	1.51	1.00
4		14.9		4	E ⇐	0.31	0.113	0.230	0.49	1.01
5		15.0		4	N ⇓	0.35	0.024	0.172	0.14	1.16
6		13.3		0	No wind	0.34	0.040	0.170	0.24	1.12
7		13.5		4	W ⇒	0.424	0.017	0.171	0.10	1.41
8		13.3	000000xxxxxxxx0	4	S ⇑	0.30	0.289	0.190	1.52	1.00
9		13.4		4	E ⇐	0.30	0.277	0.244	1.13	1.00
10		13.3		4	N ⇓	0.30	0.152	0.244	0.62	1.00

*) 0 – closed; x – open

The simulation results show the significant impact of the wind on ice jam formation. It is a logical consequence of the backwater effect that causes an increase in depth and a decrease in water velocity in the direct vicinity of the dam. In such conditions, the wind develops the main drag force on the surface ice transport. Thus, while the wind is blowing in the same direction as that of the water flow, it causes the ice to run with a speed exceeding the downstream water velocity. In such a case, the ice is pushed towards the dam, and no ice stoppage is observed at the southern shore of the island (see cases 3, 8 and 9 in the Table 6). This is clearly visible for a southern wind, but also for an eastern one. However, in this case, the order of opening the spans of the spillway will have an impact on the ice transport. Meanwhile, wind blowing from the opposite direction (west) to the water flow leads to the ice stoppage and jamming (Figure 16). Due to the fact that the water drag is not high, the accumulation is not very thick without a clear location of toe; however, the ice run proceeds with low velocity ($V_i/V_w < 0.15$). Thus, the ice accumulation propagates upstream of the reservoir; even though, it developes in a juxtaposed ice form due to the low water drag.

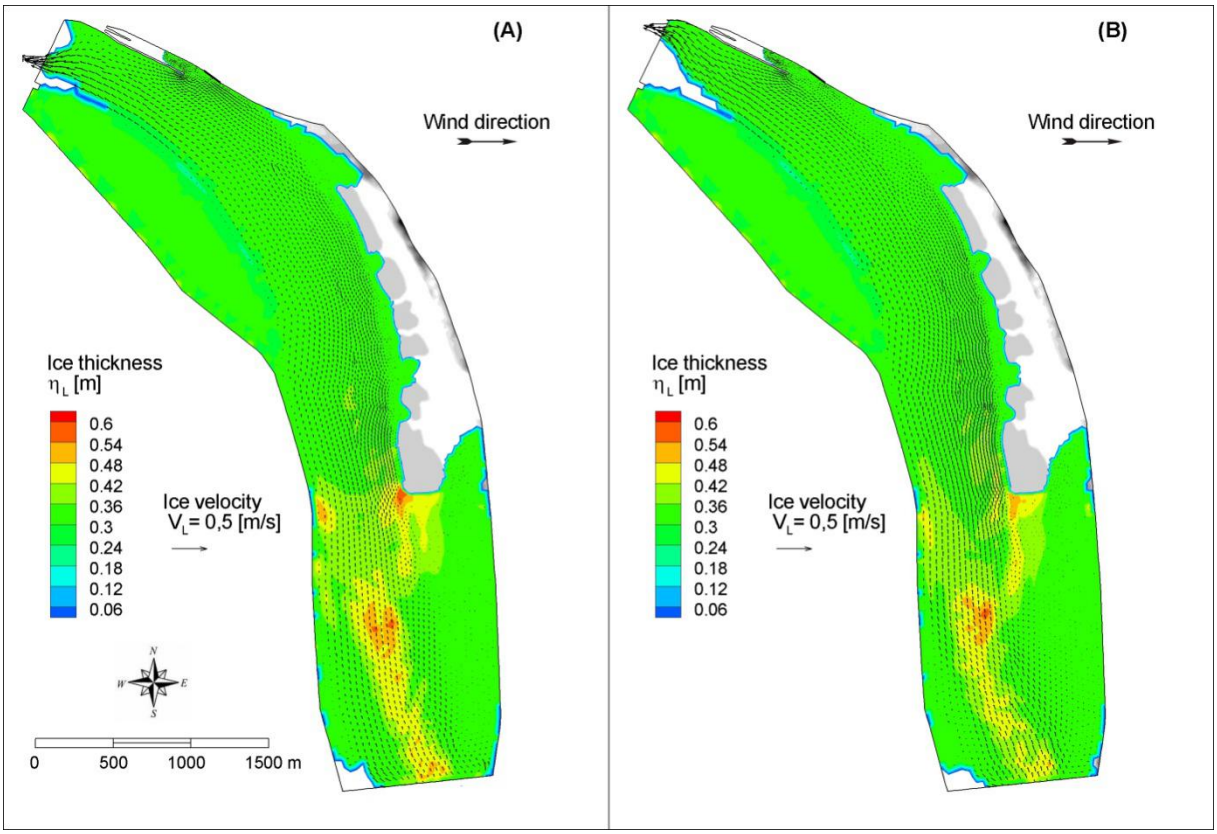

635

636 **Figure 16 Ice thickness and ice velocity distribution in the downstream area of the reservoir for the water discharge Q =**
637 **1308 m³/s and variable spillway span opening: left (a) and right spans (b)**

638 The abovementioned situation with the eastern wind, as well as the case with the northern wind are
639 affected by the spillway operation. Even though, the distance from the spillway to the area of
640 interest is about 4 kilometers, the reduction in ice sluicing caused by opening the wrong spillway
641 sections enables ice accumulation to happen upstream. Since the water velocity at the reservoir is
642 significantly reduced due to the backwater effect, the main mechanism affecting the ice flow at the
643 direct vicinity of the spillway will be the wind. For an eastern wind, although intact ice covers the
644 area on the left bank, ice drifts away from the opened sections of the spillway towards the west
645 bank. Consequently, less ice will pass the dam, and its movement will be hampered in the entire
646 reservoir. It was shown in Table 6 that the ice velocity is reduced, but the thickness did not increase
647 from the single floe thickness. For this reason, it must be noted that the span opening configuration
648 will mainly be determined by the ice dynamic in the reservoir and its inflow towards the spillway,
649 together with the wind direction.

650 The ice jam commonly happens during the low flow condition that may not necessarily lead to the
651 risk of flooding due to the low discharge. However, in the case of not releasing the ice jam in the
652 warm spell of spring, increased discharge resultant from the snow melting may cause flooding
653 damages.

654 ## 3 Conclusion

655 In determining the ice jam potential for rivers that are subjected to the extensive engineering works,
656 it is important to predict and eliminate possible risk (Shen, 2016). The proposed methodology,
657 because of the minimum user interference, excludes introspective errors. However, it does not
658 undermine the already existing practices. As shown by the examples, the obtained results clearly
659 determine and assess the potential ice jamming that arises from the proposed engineering works.
660 Considering the Odra River flood management project, the possibility of ice jam formation resulting
661 from the river engineering works in the Słubice area is increased if an ice run of high concentration
662 occurs during average flow conditions. While the risk of ice jamming during the low flow conditions is
663 reduced. It should also be noted that the formation of a main channel with a relatively uniform depth
664 will greatly enhance the ice-breaking operation. Although jams may form to a greater extent, they
665 will be easier to release. The application of the mathematical model to the proposed reservoir on the
666 Vistula River in the scope of the ice dynamics, has been a success, because it helped to deliver on two
667 very important targets: establishing frames for ice sluicing operations, and redeveloping the artificial
668 islands. Processing the numerical model results according to the presented methodology contributed
669 to the designation of areas prone to ice jamming and the level of the related risk assessment.

670 Regarding the proposed water management plan for the ice sluicing target, based on the proposed
671 results, it is needed to take into account the hydrological and meteorological conditions that are
672 simulated in the study. Furthermore, since results show a potential ice stoppage based on the shape
673 of the islands, a practical solution would be to redesigning the islands into more rounded shapes.

This newly presented method embrace a wide type of inland water areas including lowland rivers and reservoirs. This approach does not perquisite the ice stoppage criteria like the location and velocity threshold. The model is based on the 2 novel methods of comparing the original and final ice thickness, and the ice velocity to the water velocity. Referring to the limitation of the approach, major required data would be mentioned; for instance, hydrodynamic, bathymetric, and ice condition data.

Acknowledgments

The bathymetry data used in the Odra River study were provided by Sweco Consulting and were part of the Odra-Vistula Flood Management Project – 8524 Pl, Sub-component 1A: Flood protection of areas in Zachodniopomorskie Voivodeship. The Vistula River study was supported by the National Water Management Authority 'Wody Polskie' Project no KZGW/KS/306/2019. The author wishes to show the appreciation to the anonymous reviewers for their careful reading of the manuscript and their many insightful comments and suggestions.

Literature

Ashton, G.D., 1986. River and lake ice engineering. Water Resources Publication, Littleton Co, USA.
Ashton, G.D., 1978. River ice. Annu. Rev. Fluid Mech. 10, 369–392.
Babiński, Z., 1982. Influence of the water dam in Włocławek on fluvial processes of the Vistula River. Polish Academy of Sciences, Institute of Geography and Spatial Organization.
Beltaos, S., 2018. The 2014 ice–jam flood of the Peace-Athabasca Delta: Insights from numerical modelling. Cold Reg. Sci. Technol. 155, 367–380.
Beltaos, S., 2003. Numerical modelling of ice-jam flooding on the Peace–Athabasca delta. Hydrol. Process. 17, 3685–3702.
Beltaos, S., 1995. River Ice Jams. Water Resources Publication.
Beltaos, S., 1983. River ice jams: theory, case studies, and applications. J. Hydraul. Eng. 109, 1338–1359.
Beltaos, S., Burrell, B.C., 2015. Hydroclimatic aspects of ice jam flooding near Perth-Andover, New Brunswick. Can. J. Civ. Eng. 42, 686–695.
Boucher, É., Bégin, Y., Arseneault, D., 2009. Impacts of recurring ice jams on channel geometry and geomorphology in a small high-boreal watershed. Geomorphology 108, 273–281.
Boucher, E., Bégin, Y., Arseneault, D., Ouarda, T.B., 2012. Long-term and large-scale river-ice processes in cold-region watersheds. Gravel-Bed Rivers Process. Tools Environ. 546–554.
Brunner, G.W., 2002. Hec-ras (river analysis system), in: North American Water and Environment Congress & Destructive Water. ASCE, pp. 3782–3787.

Carson, R., Beltaos, S., Groeneveld, J., Healy, D., She, Y., Malenchak, J., Morris, M., Saucet, J.-P., Kolerski, T., Shen, H.T., 2011. Comparative testing of numerical models of river ice jams. Can. J. Civ. Eng. 38, 669–678. https://doi.org/10.1139/l11-036

Das, A., Lindenschmidt, K.-E., 2020. Evaluation of the sensitivity of hydraulic model parameters, boundary conditions and digital elevation models on ice-jam flood delineation. Cold Reg. Sci. Technol. 103218.

Flato, G., Gerard, R., 1986. Calculation of ice jam thickness profiles, in: Proc., 4th Workshop on Hydr. of River Ice. pp. 1–25.

Gosztowtt, J., 2018. Spatio-temporal changes of Vistula riverbed below the W\loc\lawek hydropower plant (MSc Thesis). University of Salzburg, Salzburg.

Grześ, M., 1991. Ice jams and floods on the lower Vistula river: mechanism and processes. Polish Academy of Sciences Institute of Geography and Spatial Organization, Warsaw.

Hicks, F.E., Steffler, P.M., Gerard, R., 1992. Finite element modeling of surge propagation and an application to the Hay River, N.W.T. Can. J. Civ. Eng. 19, 454–462. https://doi.org/10.1139/l92-055

Ji, S., Shen, H.T., Wang, Z., Shen, H.H., Yue, Q., 2005. A viscoelastic-plastic constitutive model with Mohr-Coulomb yielding criterion for sea ice dynamics. ACTA Oceanol. Sin.-Engl. Ed.- 24, 54.

Kandamby, A., Jayasundara, N., Shen, H.T., Deyhle, C., 2010. A numerical river ice model for Elbe River, in: 20th IAHR International Symposium on Ice. Lahti, Finland. Lahti, Finland.

Knack, I.M., Shen, H.T., 2018. A numerical model for sediment transport and bed change with river ice. J. Hydraul. Res. 56, 844–856.

Knack, I.M., Shen, H.T., 2017. Numerical modeling of ice transport in channels with river restoration structures. Can. J. Civ. Eng. 44, 813–819. https://doi.org/10.1139/cjce-2017-0081

Knack, I.M., Shen, H.T., 2016. A numerical model study on Saint John River ice breakup. Can. J. Civ. Eng. 45, 817–826.

Kolerski, T., 2018. Mathematical modeling of ice dynamics as a decision support tool in river engineering. Water 10, 1241.

Kolerski, T., 2016. Modeling of Ice Passage Through Reservoirs System on the Vistula River, in: Rowiński, P., Marion, A. (Eds.), Hydrodynamic and Mass Transport at Freshwater Aquatic Interfaces: 34th International School of Hydraulics, GeoPlanet: Earth and Planetary Sciences. Springer International Publishing, Cham, pp. 35–47. https://doi.org/10.1007/978-3-319-27750-9_4

Kolerski, T., Huang, F., Shen, H.T., 2016. Development of Ice Jam Toe Configurations. Presented at the 23 rd IAHR International Symposium on Ice, Ann Arbor, Michigan USA,.

Kolerski, T., Shen, H.T., 2015. Possible effects of the 1984 St. Clair River ice jam on bed changes. Can. J. Civ. Eng. 42, 696–703.

Kovachis, N., Burrell, B.C., Huokuna, M., Beltaos, S., Turcotte, B., Jasek, M., 2017. Ice-jam flood delineation: Challenges and research needs. Can. Water Resour. JournalRevue Can. Ressour. Hydr. 42, 258–268.

Kreft, A., Parzonka, W., 2007. Issues related to the modernization of river regulation structures on the border section of the Lower Odra river. Infrastruct. Ecol. Rural Areas 123–134.

Lal, A.W., Shen, H.T., 1991. Mathematical model for river ice processes. J. Hydraul. Eng. 117, 851–867.

Lindenschmidt, K.-E., Carstensen, D., Fröhlich, W., Hentschel, B., Iwicki, S., Kögel, M., Kubicki, M., Kundzewicz, Z.W., Lauschke, C., \Lazarów, A., 2019. Development of an Ice Jam Flood Forecasting System for the Lower Oder River—Requirements for Real-Time Predictions of Water, Ice and Sediment Transport. Water 11, 95.

Lindenschmidt, K.E., Rokaya, P., 2019. A Stochastic Hydraulic Modelling Approach to Determining the Probable Maximum Staging of Ice-Jam Floods. J. Environ. Inform. 34.

Lindenschmidt, K.-E., Sydor, M., Carson, R.W., 2012. Modelling ice cover formation of a lake–river system with exceptionally high flows (Lake St. Martin and Dauphin River, Manitoba). Cold Reg. Sci. Technol. 82, 36–48.

759 Liu, L., Shen, H.T., 2005. Numerical modeling of 2003 Grasse River ice jam and scenario analysis.
760 Presented at the Proc., 13th Workshop of the Hydraulics of Ice Covered Rivers, Hanover, NH,
761 USA.
762 Marszelewski, W., Pawłowski, B., 2019. Long-Term Changes in the Course of Ice Phenomena on the
763 Oder River along the Polish–German Border. Water Resour. Manag. 33, 5107–5120.
764 https://doi.org/10.1007/s11269-019-02417-2
765 Mudelsee, M., Börngen, M., Tetzlaff, G., Grünewald, U., 2004. Extreme floods in central Europe over
766 the past 500 years: Role of cyclone pathway "Zugstrasse Vb." J. Geophys. Res. Atmospheres
767 109.
768 Pariset, E., Hauser, R., 1961. FORMATION AND EVOLUTION OF ICE COVERS ON RIVERS. Trans. Eng.
769 Inst. Can. 5, 41–49.
770 Pariset, E., Hausser, R., Gagnon, A., 1966. Formation of Ice Covers and Ice Jams in Rivers. J. Hydraul.
771 Div. 92, 1–24.
772 Pawłowski, B., 2019. Ice Jams: Causes and Effects, in: Encyclopedia of Water. American Cancer
773 Society, pp. 1–9. https://doi.org/10.1002/9781119300762.wsts0035
774 Pawłowski, B., 2015. Determinants of change in the duration of ice phenomena on the Vistula River
775 in Toruń. J. Hydrol. Hydromech. 63. https://doi.org/10.1515/johh-2015-0017
776 Prowse, T.D., 1990. Heat and mass balance of an ablating ice jam. Can. J. Civ. Eng. 17, 629–635.
777 Rădoane, M., Ciaglic, V., Rădoane, N., 2010. Hydropower impact on the ice jam formation on the
778 upper Bistrita River, Romania. Cold Reg. Sci. Technol. 60, 193–204.
779 https://doi.org/10.1016/j.coldregions.2009.10.006
780 RWMA, 2010. Icebreaking operation 2009/2010 report. Regional Water Management Authority in
781 Szczecin, Szczecin.
782 RWMA, W., 2009. Instruction of icebreaking and ice sluicing thorough Włocławek Dam (No. XI).
783 Reginal Water Management Authority, Warszawa.
784 Schneck, C.C., Ghobrial, T.R., Loewen, M.R., 2019. Laboratory study of the properties of frazil ice
785 particles and flocs in water of different salinities. Cryosphere 13.
786 Shen, H.T., 2016. River Ice Processes, in: Wang, L.K., Yang, C.T., Wang, M.-H.S. (Eds.), Advances in
787 Water Resources Management. Springer International Publishing, Cham, pp. 483–530.
788 https://doi.org/10.1007/978-3-319-22924-9_9
789 Shen, H.T., 2010. Mathematical modeling of river ice processes. Cold Reg. Sci. Technol. 62, 3–13.
790 https://doi.org/10.1016/j.coldregions.2010.02.007
791 Shen, H.T., Gao, L., Kolerski, T., Liu, L., 2008. Dynamics of Ice Jam Formation and Release. J. Coast.
792 Res. 52, 25–32. https://doi.org/10.2112/1551-5036-52.sp1.25
793 Shen, H.T., Jayasundara, N.C., Tuthill, A.M., Mihm, J.E., 2005. Frequency and Severity of Past Ice Jams
794 on the Grass River. Presented at the 13 th Workshop on the Hydraulics of Ice Covered Rivers,
795 Hanover, NH, USA, p. 8.
796 Shen, H.T., Liu, L., 2003. Shokotsu River ice jam formation. Cold Reg. Sci. Technol. 37, 35–49.
797 Shen, H.T., Shen, H., Tsai, S.-M., 1990. Dynamic transport of river ice. J. Hydraul. Res. 28, 659–671.
798 Shen, H.T., Su, J., Liu, L., 2000. SPH Simulation of River Ice Dynamics. J. Comput. Phys. 165, 752–770.
799 https://doi.org/10.1006/jcph.2000.6639
800 Staśko, S., Buczyński, S., 2018. Drought and its effects on spring discharge regimes in Poland and
801 Germany during the 2015 drought. Hydrol. Sci. J. 63, 741–751.
802 https://doi.org/10.1080/02626667.2018.1446215
803 Su, J., Shen, H.T., Crissman, R.D., 1997. Numerical study on ice transport in vicinity of Niagara River
804 hydropower intakes. J. Cold Reg. Eng. 11, 255–270.
805 Svensson, U., Billfalk, L., Hammar, L., 1989. A mathematical model of border-ice formation in rivers.
806 Cold Reg. Sci. Technol. 16, 179–189.
807 Szydlowski, M., Gąsiorowski, D., Szymkiewicz, R., Zima, P., Hakiel, J., 2015. Hydropower potential of
808 the lower Vistula. Acta Energ. 1, 18–25.

809 Szydlowski, M., Kolerski, T., 2018. Numerical Modeling of Water and Ice Dynamics for Analysis of
810 Flow Around the Kiezmark Bridge Piers, in: Free Surface Flows and Transport Processes.
811 Springer, pp. 465–476.
812 Szymkiewicz, R., 2017. Dolna Wisła-rzeka niewykorzystanych możliwości. Wydawnictwo Politechniki
813 Gdańskiej.
814 Thériault, I., Saucet, J.-P., Taha, W., 2010. Validation of the Mike-Ice model simulating river flows in
815 presence of ice and forecast of changes to the ice regime of the Romaine river due to
816 hydroelectric project, in: Proceedings of the 20th IAHR International Symposium on Ice,
817 Lahti, Finland.
818 Timalsina, N.P., Charmasson, J., Alfredsen, K.T., 2013. Simulation of the ice regime in a Norwegian
819 regulated river. Cold Reg. Sci. Technol. 94, 61–73.
820 Timoney, K., Peterson, G., Fargey, P., Peterson, M., McCanny, S., Wein, R., 1997. Spring ice-jam
821 flooding of the Peace-Athabasca Delta: Evidence of a climatic oscillation. Clim. Change 35,
822 463–483.
823 Tuthill, A., Ashton, G., Hendershot, P., Quadrini, J., 2008. Grasse River Ice Control Structure, Physical
824 Model Study. Presented at the 19th IAHR International Symposium on Ice, Vancouver, BC,
825 Canada, p. 11.
826 Uzuner, M.S., Kennedy, J.F., 1976. Theoretical model of river ice jams. J. Hydraul. Div. 102.
827 Uzuner, M.S., Kennedy, J.F., 1974. Hydraulics and mechanics of river ice jams. IOWA INST OF
828 HYDRAULIC RESEARCH IOWA CITY.
829 Wang, J., Shi, F., Chen, P., Wu, P., Sui, J., 2015. Impact of bridge pier on the stability of ice jam. J.
830 Hydrodyn. 27, 865–871. https://doi.org/10.1016/S1001-6058(15)60549-2
831 White, K.D., 1999. Hydraulic and physical properties affecting ice jams.
832 Wolfe, B.B., Hall, R.I., Wiklund, J.A., Kay, M.L., 2020. Past variation in Lower Peace River ice-jam flood
833 frequency. Environ. Rev. 1–9.
834 Wolski, K., Tymiński, T., Głuchowska, B., 2017. Analysis of ice phenomena hazard on the middle Odra
835 river. Ann. Wars. Univ. Life Sci. – SGGW Land Reclam. 49. https://doi.org/10.1515/sggw-
836 2017-0024
837 Wu, J., 1973. Prediction of near-surface drift currents from wind velocity. J. Hydraul. Div. 99, 1291–
838 1302.

839